

IRS-assisted Multi-cell Multi-band Systems: Practical Reflection Model and Joint Beamforming Design

Wenhao Cai, Rang Liu, *Graduate Student Member, IEEE*, Ming Li, *Senior Member, IEEE*,
Yang Liu, *Member, IEEE*, Qingqing Wu, *Senior Member, IEEE*, and Qian Liu, *Member, IEEE*

Abstract—Intelligent reflecting surface (IRS) has been regarded as a promising and revolutionary technology for future wireless communication systems owing to its capability of tailoring signal propagation environment in an energy/spectrum/hardware-efficient manner. However, most existing studies on IRS optimizations are based on a simple and ideal reflection model that is impractical in hardware implementation, which thus leads to severe performance loss in realistic wideband/multi-band systems. To deal with this problem, in this paper we first propose a more practical and more tractable IRS reflection model that describes the difference of reflection responses for signals at different frequencies. Then, we investigate the joint transmit beamforming and IRS reflection beamforming design for an IRS-assisted multi-cell multi-band system. Both power minimization and sum-rate maximization problems are solved by exploiting popular second-order cone programming (SOCP), Riemannian manifold, minimization-majorization (MM), weighted minimum mean square error (WMMSE), and block coordinate descent (BCD) methods. Simulation results illustrate the significant performance improvement of our proposed joint transmit beamforming and reflection design algorithms based on the practical reflection model in terms of power saving and rate enhancement.

Index Terms—Intelligent reflecting surface, practical reflection model, multi-cell multi-band systems, beamforming optimization.

I. INTRODUCTION

With the rapid development of wireless communication networks and the popularizing of various intelligent devices, the demands for high transmission rate and low latency have also been exponentially growing in the last decades [1]. To accommodate these constantly increasing demands, several key technologies, such as heterogeneous dense networks, massive multiple-input multiple-output (MIMO), and millimeter-wave (mmWave) communications, have been proposed to improve system performance for the fifth-generation (5G) and beyond communication networks [2], [3]. However, it seems that we are approaching the limit of the theories obtained from such technologies. Furthermore, the required high hardware complexity and consequently high energy consumption in

practical implementations remain the bottlenecks for large-scale deployment [4]. Therefore, new technologies are desired to provide fundamental advances for future wireless networks in a more energy/spectrum/hardware-efficient fashion.

The innovative concept of intelligent reflecting surface (IRS) has recently emerged as such a promising technology [4]-[10]. An IRS is a two-dimensional (2D) planar array consisting of numerous reflecting elements, which are implemented by reconfigurable electromagnetic (EM) internals with very low power consumption. Each reflecting element independently adjusts the phase-shift and amplitude of incident EM waves in a programmable manner, which collaboratively achieves reflection beamforming and reshapes propagation environments for wireless communications. Deploying an IRS in existing communication networks brings the capability of creating a favorable propagation environment and provides more degrees of freedom (DoFs) for network optimizations. Furthermore, these lightweight, hardware-efficient, and cost-effective reflecting elements provide the IRS with portability and mobility for various practical applications and enable large-scale IRSs to produce higher passive beamforming gains to significantly improve the transmission quality of service (QoS). Therefore, IRS has been envisioned as a revolutionary technology owing to its capability of creating a smart and reconfigurable wireless propagation environment in a hardware-efficient way and has drawn significant attentions within both industry and academic communities [4].

In order to take advantage of the IRS mentioned above, extensive researches on deploying IRS in various wireless communication systems have been conducted to improve the performance under different metrics. By judiciously adjusting IRS elements, the reflected signals are intelligently elaborated to achieve performance improvement in terms of spectral efficiency [11], energy efficiency [12], transmit power [13], [14], sum-rate [15]-[17], etc., for single-user/multi-user MIMO/multi-input single-output (MISO) [11]-[16], wideband orthogonal frequency division multiplexing (OFDM) [17], or multi-cell systems [18]. In addition, researchers have explored the designs of IRS with low-resolution phase-shift [19] and phase error [20] or under imperfect channel state information (CSI) [21]. Moreover, IRS has been applied in various novel applications, such as physical layer security [22], [23], index modulation [24], passive information transmission [25], etc.

In the above applications, it is assumed that each reflecting element has an ideal IRS reflection model, which induces the

W. Cai, R. Liu, M. Li, and Y. Liu are with the School of Information and Communication Engineering, Dalian University of Technology, Dalian 116024, China (e-mail: wenhaocai@mail.dlut.edu.cn; liurang@mail.dlut.edu.cn; mli@dlut.edu.cn; yangliu_613@dlut.edu.cn).

Q. Wu is with the State Key Laboratory of Internet of Things for Smart City, University of Macau, Macau 999078, China (email: qingqingwu@um.edu.mo).

Q. Liu is with the School of Computer Science and Technology, Dalian University of Technology, Dalian 116024, China (e-mail: qianliu@dlut.edu.cn).

same constant amplitude yet variable phase-shift response to the incident signals. Based on this ideal IRS reflection model, a lot of existing algorithms, e.g., majorization minimization (MM), Riemannian manifold optimization, semidefinite relaxation (SDR), etc., have been readily employed in IRS reflection optimizations. Unfortunately, such an ideal IRS is difficult to be realized by current hardware circuit techniques. Therefore, existing designs with the ideal reflection model inevitably suffer from severe performance loss in realistic systems since the responses of practical hardware circuits are quite different from the ideal one [26]-[30].

In order to unlock the full potential IRS in realistic systems, many different practical IRS reflection models are derived to illustrate the mechanism that affects the reflection coefficient [26]-[29], [31]. The seminal work [26] presented a two-dimensional amplitude-phase reflection model, which shows a fundamental relationship between the reflection amplitude and phase-shift for narrowband systems. However, it has been verified that the reflection amplitude and phase-shift vary with the frequency of incident signals [27]. This two-dimensional reflection model, which does not consider the effect of signal frequency, cannot be readily applied in wideband/multi-band systems. To tackle this issue, in our previous work [28], we analyzed the responses to signals at different frequencies and established a three-dimensional amplitude-frequency-phase reflection model. Since this sophisticated model brings huge difficulties for joint beamforming and reflection designs, a simplified version was developed in [29] for typical wideband OFDM systems. Besides, the authors in [31] derived a more general reflection model using rigorous scattering parameter network analysis, which mainly focuses on simple IRS-aided communication systems and thus leads to a complicated model for a certain complicated communication system, e.g., the multi-cell multi-band system considered in this paper. Therefore, the existing IRS reflection model is too complicated to be used for the joint beamforming and IRS reflection designs. Deriving a more straightforward and more tractable practical IRS reflection model for the multi-cell multi-band systems remains an open problem.

Motivated by the above, in this paper we propose a simplified practical IRS reflection model for IRS-assisted multi-cell multi-band systems and then investigate associated joint transmit beamforming and IRS reflection beamforming designs. Specifically, multiple base stations (BSs), which belong to the same service provider but operate at different frequency bands, simultaneously serve the users in their cells with the aid of one IRS. To the best of our knowledge, this problem has not been investigated in the literature yet. Our main contributions are summarized as follows.

- We first analyze the IRS phase-shift response to the incident signals at different frequencies and provide a lean practical frequency-dependent IRS reflection model. Compared with our previous work, this newly proposed model significantly reduces the required computational complexity and is more suitable for realistic multi-cell multi-band systems.
- Then, we investigate the power minimization problem, which aims to minimize the total transmit power sub-

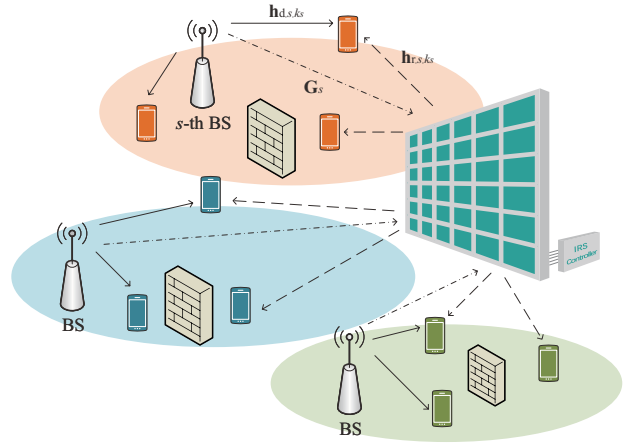


Fig. 1: An IRS-assisted multi-cell multi-band system.

ject to the signal-to-interference-plus-noise ratio (SINR) constraints of all users and the practical IRS reflection model. A three-step algorithm is proposed to solve for the transmit beamforming and the practical IRS reflection beamforming by utilizing the second-order cone programming (SOCP), the Riemannian manifold optimization, and the minimization-majorization (MM) method after some sophisticated transformations.

- The sum-rate maximization problem is also investigated to maximize the sum-rate subject to the total transmit power constraint and the practical IRS reflection model. In order to effectively handle this non-convex problem, we exploit the weighted minimum mean square error (WMMSE) approach to convert the original problem into a solvable multi-variable optimization, which is then handled by the block coordinate descent (BCD) method. Based on the proposed lean practical frequency-phase model, the closed-form solutions of IRS phase-shift and service selection of each element can be simultaneously obtained for the sum-rate maximization problem, which can significantly improve the efficiency of the algorithm.
- Finally, extensive simulation results are illustrated to show the effectiveness of our proposed algorithms and validate the significant performance improvement achieved by considering the proposed practical IRS reflection model in the designs for multi-cell multi-band communication networks.

Notation: Boldface lower-case and upper-case letters indicate column vectors and matrices, respectively. \mathbb{C} and \mathbb{R}^+ denotes the set of complex and positive real numbers, respectively. $(\cdot)^*$, $(\cdot)^T$, $(\cdot)^H$, and $(\cdot)^{-1}$ denote the conjugate, transpose, conjugate-transpose operations, and the inversion of a matrix, respectively. $\mathbb{E}\{\cdot\}$ and $\Re\{\cdot\}$ denote statistical expectation and the real part of a complex number, respectively. \mathbf{I}_L indicates an $L \times L$ identity matrix. $\|\mathbf{a}\|$ and $\|\mathbf{a}\|_0$ denote the ℓ_2 norm and ℓ_0 norm of a vector \mathbf{a} , respectively. \odot denotes the Hadamard product. In addition, $\angle\theta$ denotes the angle of a complex number θ .

II. SYSTEM MODEL AND PRACTICAL REFLECTION MODEL

A. System Model

We consider an IRS-assisted multi-cell multi-band wireless communication system as shown in Fig. 1, where an IRS composed of M reflecting elements is deployed to simultaneously assist the downlink communications in S cells. Specifically, in the s -th cell, $s = 1, 2, \dots, S$, the BS equipped with N_t transmit antennas serves K_s single-antenna users at the frequency f_s . Let $\mathcal{S} \triangleq \{1, \dots, S\}$ denote the set of BSs, $\mathcal{K}_s \triangleq \{1, \dots, K_s\}$ denote the set of the users served by the s -th BS, and $\mathcal{M} \triangleq \{1, \dots, M\}$ denote the set of IRS reflecting elements. Without loss of generality, we assume $f_1 > f_2 > \dots > f_S$ in the considered multi-cell multi-band system. In addition, the IRS is controlled by an IRS controller through a dedicated control link and only the first-order reflection is considered due to significant path loss.

Denote $\mathbf{z}_s \triangleq [z_{s,1}, \dots, z_{s,K_s}]^T \in \mathbb{C}^{K_s}$ as the transmitted symbols for the users served by the s -th BS, $\mathbb{E}\{\mathbf{z}_s \mathbf{z}_s^H\} = \mathbf{I}_{K_s}$, and $\mathbf{W}_s \triangleq [\mathbf{w}_{s,1}, \dots, \mathbf{w}_{s,K_s}] \in \mathbb{C}^{N_t \times K_s}$ as the precoder matrix of the s -th BS, $\forall s \in \mathcal{S}, k_s \in \mathcal{K}_s$. Since the BSs operate at different frequencies, the inter-cell interference can be easily eliminated through receiving filters at the users. Thus, the received baseband signal at the k_s -th user served by the s -th BS can be expressed as

$$y_{s,k_s} = (\mathbf{h}_{r,s,k_s}^H \Theta_s \mathbf{G}_s + \mathbf{h}_{d,s,k_s}^H) \sum_{k_s \in \mathcal{K}_s} \mathbf{w}_{s,k_s} z_{s,k_s} + n_{s,k_s}, \quad (1)$$

where $\mathbf{h}_{r,s,k_s} \in \mathbb{C}^M$, $\mathbf{G}_s \in \mathbb{C}^{M \times N_t}$, and $\mathbf{h}_{d,s,k_s} \in \mathbb{C}^{N_t}$ represent the baseband equivalent channels from the IRS to the k_s -th user, from the s -th BS to the IRS, and from the s -th BS to the k_s -th user, respectively. It is noted that the quasi-static flat-fading Rayleigh channel model¹ is adopted for all channels and we assume that all the CSIs are perfectly known at the BSs given existing efficient channel estimation approaches [32]-[39]. For example, the CSIs can be acquired at different BSs based on the received pilot signals from their users with acceptable training overhead. $n_{s,k_s} \sim \mathcal{CN}(0, \sigma^2)$ denotes the additive white Gaussian noise (AWGN) at the k_s -th user. $\Theta_s \triangleq \text{diag}\{\theta_s\}$, and $\theta_s \triangleq [\theta_{s,1}, \dots, \theta_{s,M}]^T$ is the IRS reflection coefficient vector for the signals transmitted by the s -th BS, i.e., the signals at the frequency f_s . We emphasize that with the same IRS settings, the IRS reflection vectors are different for the incident signals at different frequencies due to practical hardware characteristics, and they are inherently correlated as described in the next subsection.

With the received signal in (1), the SINR of the k_s -th user served by the s -th BS is given by

$$\gamma_{s,k_s} = \frac{|\mathbf{h}_{r,s,k_s}^H \Theta_s \mathbf{G}_s + \mathbf{h}_{d,s,k_s}^H \mathbf{w}_{s,k_s}|^2}{\sum_{j \in \mathcal{K}_s, j \neq k_s} |\mathbf{h}_{r,s,k_s}^H \Theta_s \mathbf{G}_s + \mathbf{h}_{d,s,k_s}^H \mathbf{w}_{s,j}|^2 + \sigma^2}. \quad (2)$$

B. Practical IRS Reflection Model

An IRS is typically implemented by a printed circuit board (PCB), in which semiconductor devices [40], e.g., positive-intrinsic-negative (PIN) diodes, are embedded to tune the

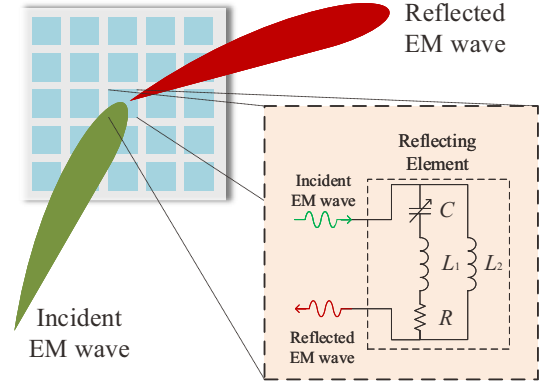


Fig. 2: The equivalent circuit of a reflecting element.

reflection response by varying the impedance of each reflecting element. As discussed in [26]-[29], the reflection response of a reflecting element can be described by an equivalent parallel resonant circuit as shown in Fig. 2, where L_1 , L_2 , C , and R denote the equivalent inductances, variable capacitance, and the loss resistance, respectively. Thus, the impedance of a reflecting element can be written as

$$Z(C, f) = \frac{j2\pi f L_1 (j2\pi f L_2 + \frac{1}{j2\pi f C} + R)}{j2\pi f L_1 + (j2\pi f L_2 + \frac{1}{j2\pi f C} + R)}. \quad (3)$$

Then, the reflection coefficient θ that describes the effect of a reflecting element on the incident EM waves is given by

$$\theta(C, f) = \frac{Z(C, f) - Z_0}{Z(C, f) + Z_0}, \quad (4)$$

where $Z_0 = 377\Omega$ denotes the free space impedance. From the microwave theory (4), we see that the reflection coefficient $\theta(C, f)$ is a function of the capacitance C and the frequency f of incident signals. In other words, the reflection coefficient of each reflecting element is controlled by the variable capacitance and the same reflecting element exhibits different amplitude and phase-shift responses to the signals at different frequencies. The creditability and correctness of the microwave theory can also be verified by the experimental and simulation results in [27], [30]. We have analyzed this phenomenon and established a sophisticated three-dimensional amplitude-frequency-phase model in our initial work [28], and further provided a simplified version for IRS optimization in wideband systems [29]. However, this practical IRS reflection model is composed of complex arc-tangent and *Witch of Agnesi* functions, which are too complicated and inconvenient for the joint beamforming and IRS reflection designs in the considered multi-cell multi-band systems. This motivates us to derive a simpler approximated reflection model.

To establish a simplified and tractable IRS reflection model, we first plot the phase-shift response $\angle\theta$ versus the capacitance in Fig. 3 according to (3) and (4). We take the scenario that $S = 3$, $f_1 = 2.605\text{GHz}$, $f_2 = 2.345\text{GHz}$, and $f_3 = 1.885\text{GHz}$ as an example², which adopts three available frequencies of

¹The proposed practical IRS reflection model and associated design algorithms are also suitable for other channel fading models, e.g., Rician fading.

²The proposed IRS reflection model can be easily extended to other frequency combinations and similar conclusions can be obtained.

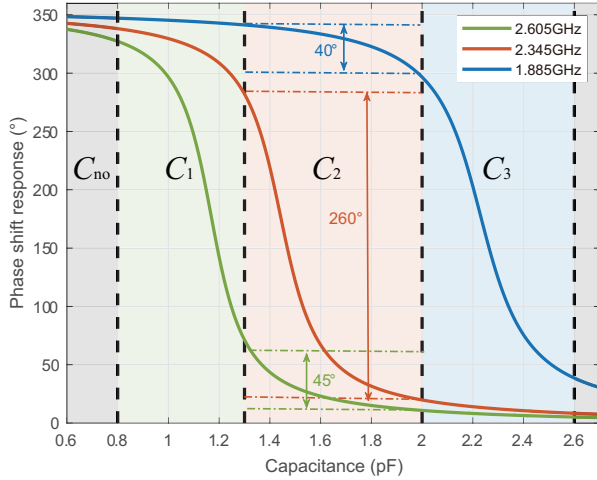


Fig. 3: The phase-shift response versus capacitance for different frequencies ($S = 3$, $f_1 = 2.605\text{GHz}$, $f_2 = 2.345\text{GHz}$, $f_3 = 1.885\text{GHz}$).

China Mobile 4G network. In addition, we choose a practical surface-mount diode SMV1231-079 [41] with parameters $L_1 = 2.5\text{nH}$, $L_2 = 0.7\text{nH}$, and $R = 1\Omega$ to implement the IRS. It can be noticed that the phase-shift response varies with the frequency of incident signal as analyzed above. In addition, we observe that for a given frequency f , the phase-shift can be accurately tuned in a specific capacitance range but maintains almost the same in other ranges. Furthermore, the tunable capacitance ranges of different frequencies are nearly not overlapped when the difference of frequencies is relatively large. In other words, when we adjust the capacitance to provide a tunable phase-shift for a certain frequency, the phase-shift response for other frequencies is almost unchanged. In this way, the capacitance values in Fig. 3 can be divided into four ranges (the green, orange, blue, and gray areas), which exhibit four different reflection responses for the signals of three different frequencies.

Take the orange area as an example. When the capacitance varies from 1.3pF to 2pF, the phase-shift response for signals at 2.345GHz changes by 260° , while 1.885GHz changes by 40° and 2.605GHz changes by 45° . Therefore, we can approximately consider this capacitance range as that the reflecting element serves the BS operating at 2.345GHz by providing an ideal $(0, 2\pi]$ phase-shift and meanwhile exhibits a fixed $0/2\pi$ phase-shift for other BSs. Since the IRS consists of lots of reflecting elements, the performance loss due to the approximation for each independent reflecting element is negligible. Moreover, considering the hardware complexity and cost in practical implementations, the tunable phase-shift values are usually discrete (e.g., 1-bit or 2-bit resolution), which also supports our approximation. Correspondingly, the green and blue areas indicate that the BSs operating at 2.605GHz and 1.885GHz are served by this reflecting element, respectively. Meanwhile, in the gray areas, IRS provides fixed and uncontrollable phase-shifts to all the BSs. Therefore, IRS cannot generate effective beamforming for any BSs.

Based on the above descriptions, we simplify the phase-shift response for different operating frequencies in Table I, where C_1 , C_2 , C_3 , and C_{no} correspond to the capacitance ranges of

TABLE I: A simplified representation of Fig. 3.

	C_1	C_2	C_3	C_{no}
2.605 GHz	$(0, 2\pi]$	0	0	$0/2\pi$
2.345 GHz	2π	$(0, 2\pi]$	0	$0/2\pi$
1.885 GHz	2π	2π	$(0, 2\pi]$	$0/2\pi$

the green, orange, blue, and gray areas in Fig. 3, respectively. We can clearly see that by controlling the capacitance of a reflecting element, a certain BS (i.e., the signal with a certain frequency) is selected to be served by this reflecting element with an ideal (i.e., $0 - 2\pi$ tunable) phase-shift meanwhile the other BSs have a fixed $0/2\pi$ phase-shift, or none of the BSs are selected. This frequency-selective characteristic of each reflecting element motivates us to describe a practical phase-shift response using the product of an ideal phase-shift and a binary indicator. This simplified IRS phase-shift response transforms the extremely complicated nonlinear functional relationship between phase-shift and frequency into a binary functional relationship, which can further facilitate the joint transmit beamforming and IRS phase-shift design. Thus, for the m -th reflecting element, we define its service selection vector as $\mathbf{a}_m \triangleq [a_{1,m}, \dots, a_{S,m}]^T$, $a_{s,m} \in \{0, 1\}$. Specifically, $a_{s,m} = 1$ indicates that the s -th BS is selected to be served with a fully tunable phase-shift response provided by the m -th reflecting element, and $a_{s,m} = 0$ represents that the m -th reflecting element exhibits a fixed $0/2\pi$ phase-shift for the s -th BS. For example, the four status in Table I can be represented by $\mathbf{a}_m = [1, 0, 0]^T$, $\mathbf{a}_m = [0, 1, 0]^T$, $\mathbf{a}_m = [0, 0, 1]^T$, and $\mathbf{a}_m = [0, 0, 0]^T$, respectively. In addition, according to the above analysis, each reflecting element can serve at most one BS. Thus, the constraint for the service selection vector of the m -th reflecting element can be expressed as

$$\|\mathbf{a}_m\|_0 \leq 1, \quad a_{s,m} \in \{0, 1\}, \quad \forall s, m. \quad (5)$$

We further define an $S \times M$ service selection matrix for the IRS as $\mathbf{A} \triangleq [\mathbf{a}_1, \dots, \mathbf{a}_M]$. It is noted that the s -th row of \mathbf{A} is also the service selection vector for the s -th BS and indicates which reflecting elements serve this BS. For brevity, we denote the service selection vector for the s -th BS as $\tilde{\mathbf{a}}_s \triangleq [a_{s,1}, \dots, a_{s,M}]^T \in \{0, 1\}^M$, which leads to

$$\mathbf{A} = [\mathbf{a}_1, \dots, \mathbf{a}_M] = [\tilde{\mathbf{a}}_1, \dots, \tilde{\mathbf{a}}_S]^T. \quad (6)$$

Denote the ideal phase-shift vector ϕ_s for the s -th BS as $\phi_s \triangleq [\phi_{s,1}, \dots, \phi_{s,M}]^T$, $\phi_{s,m} \in (0, 2\pi]$. The practical phase-shift $\angle\theta_s$ is thus given by

$$\angle\theta_s = \phi_s \odot \tilde{\mathbf{a}}_s. \quad (7)$$

Besides, as shown in [26]-[29], the reflection amplitude also varies with the frequency of signals. However, for the signals at a certain frequency, i.e., transmitted by a certain BS, each reflecting element has the same reflection amplitude degradation, which can be compensated at the transmitter side using some advanced hardware techniques [42]. Therefore, neglecting the practical reflection amplitude response will not affect the optimizations for the considered multi-cell multi-band systems. In this way, the practical reflection vector for

the s -th BS can be written as $\boldsymbol{\theta}_s = \exp(j\angle\boldsymbol{\theta}_s)$. In summary, the practical IRS reflection model is formulated as

$$\boldsymbol{\theta}_s = \exp(j\phi_s \odot \tilde{\mathbf{a}}_s), \quad \forall s, \quad (8a)$$

$$\phi_{s,m} \in (0, 2\pi], \quad \forall s, m, \quad (8b)$$

$$\|\mathbf{a}_m\|_0 \leq 1, \quad a_{s,m} \in \{0, 1\}, \quad \forall s, m. \quad (8c)$$

Given the above system model and practical IRS reflection model, the joint transmit beamforming and IRS reflection designs for the power minimization and sum-rate maximization problems will be investigated in Sec. III and Sec. IV, respectively.

III. ALGORITHM FOR POWER MINIMIZATION PROBLEM

In this section, we aim to jointly optimize the transmit beamformers $\mathbf{W} \triangleq [\mathbf{W}_1, \dots, \mathbf{W}_S]$ for all BSs, the ideal IRS phase-shifts $\Phi \triangleq [\phi_1, \dots, \phi_S]$ for all BSs, and the service selection matrix \mathbf{A} to minimize the total transmit power, subject to users' SINR requirements and the practical reflection model. Therefore, the power minimization problem is formulated as

$$\min_{\mathbf{W}, \Phi, \mathbf{A}} \sum_{s \in \mathcal{S}} \sum_{k_s \in \mathcal{K}_s} \|\mathbf{w}_{s,k_s}\|^2 \quad (9a)$$

$$\text{s.t. } \gamma_{s,k_s} \geq \Gamma_{s,k_s}, \quad \forall s, k_s, \quad (9b)$$

$$\boldsymbol{\theta}_s = \exp(j\phi_s \odot \tilde{\mathbf{a}}_s), \quad \forall s, \quad (9c)$$

$$\phi_{s,m} \in (0, 2\pi], \quad \forall s, m, \quad (9d)$$

$$\|\mathbf{a}_m\|_0 \leq 1, \quad a_{s,m} \in \{0, 1\}, \quad \forall s, m, \quad (9e)$$

where $\Gamma_{s,k_s} > 0$ denotes the minimum SINR requirement of the k_s -th user served by the s -th BS. The non-convex NP-hard problem (9) is very difficult to solve due to the following three reasons. First, the coupled variables brought by the constraints (9b) and (9c) make this multi-variable problem hard to solve. Second, the frequency-selective model introduced by the constraint (9c) causes significant difficulty to the IRS phase-shift design. Third, the practical reflection responses for different BSs are different and related by a binary service selection matrix in constraints (9c)-(9e). In order to tackle these difficulties, we utilize the characteristics of the proposed practical reflection model to decompose the original problem (9) into two sub-problems and develop a three-step algorithm to solve the original problem as presented below.

As described in Sec. II-B, by tuning the capacitance, each reflecting element independently selects at most one BS to provide an ideal/tunable phase-shift. This fact motivates us to decompose the original problem into service selection design and the joint transmit beamforming, ideal phase-shift design sub-problems. In particular, in order to better evaluate the ability of each BS in exploiting IRS and determine the service selection, we first assume that the IRS is ideal/tunable for all BSs (i.e., $\tilde{\mathbf{a}}_s = \mathbf{1}, \forall s$) and jointly design the transmit beamforming and ideal phase-shifts for each BS. Then, the service selection matrix \mathbf{A} is optimized to select appropriate reflecting elements for serving each BS. Finally, with the obtained \mathbf{A} the ideal phase-shifts of selected reflecting elements and associated transmit beamforming are jointly designed for each BS. It is noted that the joint transmit beamforming and

ideal phase-shift design with ideal IRS reflection model (i.e., $\mathbf{A} = \mathbf{1}$) or the practical IRS reflection model follows the same route, which is presented in Sec. III-A in details. In addition, the procedure of the service selection design is described in Sec. III-B.

A. Joint Transmit Beamforming and Ideal Phase-Shift Design

Based on the above analysis, with fixed \mathbf{A} (i.e., $\tilde{\mathbf{a}}_s = \mathbf{1}, \dots, S$), the joint transmit beamforming and ideal phase-shift optimization problem for the s -th BS can be expressed as

$$\min_{\mathbf{w}_s, \phi_s} \sum_{k_s \in \mathcal{K}_s} \|\mathbf{w}_{s,k_s}\|^2 \quad (10a)$$

$$\text{s.t. } \gamma_{s,k_s} \geq \Gamma_{s,k_s}, \quad \forall k_s, \quad (10b)$$

$$\boldsymbol{\theta}_s = \exp(j\phi_s \odot \tilde{\mathbf{a}}_s), \quad (10c)$$

$$\phi_{s,m} \in (0, 2\pi], \quad \forall m. \quad (10d)$$

Before solving this problem, we present a sufficient condition for the feasibility of problem (10). If the equivalent channels $\mathbf{G}_s^H \mathbf{H}_{r,s} + \mathbf{H}_{d,s}, \forall s$ are full rank, where $\mathbf{H}_{d,s} \triangleq [\mathbf{h}_{d,s,1}, \dots, \mathbf{h}_{d,s,K_s}] \in \mathbb{C}^{N_t \times K_s}$ and $\mathbf{H}_{r,s} \triangleq [\mathbf{h}_{r,s,1}, \dots, \mathbf{h}_{r,s,K_s}] \in \mathbb{C}^{M \times K_s}$, then problem (10) is feasible for any finite QoS requirement Γ_{k_s} . The specific proof is shown in *Proposition 1* in [13]. Note that this full rank assumption has been widely adopted in the literature [17], [19], [21]. In fact, the channel coefficient matrix always satisfies full rank, when it follows some continuous independently identical distributions (i.i.d.), e.g. Rayleigh or Ricing. Therefore, in this paper, we also assume that the equivalent channels are full rank and consequently problem (10) is feasible. Moreover, some special cases that any equivalent channel is low rank, the problem can also be handled by finding a suitable initial point or the method in [43].

Notice that problem (10) is a non-convex problem due to the coupled variables in constraint (10b) and the non-convex reflection constraint (10c). Therefore, we utilize the BCD method to iteratively solve for \mathbf{W}_s and ϕ_s , which is described in the rest of this subsection.

1) *Update \mathbf{W}_s* : Given the service selection matrix \mathbf{A} and the ideal phase-shift vector ϕ_s , the practical IRS reflection vector $\boldsymbol{\theta}_s$ is fixed. Thus, the combined effective channel from the s -th BS to the k_s -th user is determined as $\mathbf{h}_{s,k_s}^H \triangleq \mathbf{h}_{r,s,k_s}^H \boldsymbol{\Theta}_s \mathbf{G}_s + \mathbf{h}_{d,s,k_s}^H$. Then, the sub-problem for optimizing \mathbf{W}_s is formulated as

$$\min_{\mathbf{w}_s} \sum_{k_s \in \mathcal{K}_s} \|\mathbf{w}_{s,k_s}\|^2 \quad (11a)$$

$$\text{s.t. } \frac{|\mathbf{h}_{s,k_s}^H \mathbf{w}_{s,k_s}|^2}{\sum_{\substack{j \in \mathcal{K}_s \\ j \neq k_s}} |\mathbf{h}_{s,k_s}^H \mathbf{w}_{s,j}|^2 + \sigma^2} \geq \Gamma_{s,k_s}, \quad \forall k_s, \quad (11b)$$

which is a standard SOCP problem and can be easily solved using the popular convex optimization toolbox such as CVX [44].

2) *Update ϕ_s* : After obtaining the transmit beamforming \mathbf{W}_s , the objective of the power minimization problem (10) is determined, which makes the IRS phase-shift design as a feasibility-check problem with lots of possible solutions,

$$\mathbf{D}_s \triangleq \sum_{k_s \in \mathcal{K}_s} \left(\widehat{\mathbf{d}}_{s,k_s,k_s} \widehat{\mathbf{d}}_{s,k_s,k_s}^H - \Gamma_{s,k_s,k_s} \sum_{\substack{j \in \mathcal{K}_s \\ j \neq k_s}} \widehat{\mathbf{d}}_{s,k_s,j} \widehat{\mathbf{d}}_{s,k_s,j}^H \right), \quad (12a)$$

$$\mathbf{b}_s \triangleq \sum_{k_s \in \mathcal{K}_s} \left[(b_{s,k_s,k_s}^* + \mathbf{1}^H \overline{\mathbf{d}}_{s,k_s,k_s}^*) \mathbf{d}_{s,k_s,k_s} - \Gamma_{s,k_s} \sum_{\substack{j \in \mathcal{K}_s \\ j \neq k_s}} (b_{s,k_s,j}^* + \mathbf{1}^H \overline{\mathbf{d}}_{s,k_s,j}^*) \mathbf{d}_{s,k_s,j} \right]. \quad (12b)$$

which may not guarantee the converge of the iteration algorithm. Therefore, another proper objective function with respect to ϕ_s is required to accelerate the convergence. A widely used method is forcing the QoS constraint (10b) to be more stricter to provide additional DoFs for the power minimization in the next iteration.

For brevity, we first define

$$\mathbf{d}_{s,k_s,j} \triangleq \text{diag}(\mathbf{h}_{\Gamma_{s,k_s}}^H) \mathbf{G}_s \mathbf{w}_{s,j}, \quad (13a)$$

$$b_{s,k_s,j} \triangleq \mathbf{h}_{\mathbf{d}_{s,k_s}}^H \mathbf{w}_{s,j}, \quad (13b)$$

and reformulate the QoS constraint (10b) as

$$\left| \boldsymbol{\theta}_s^T \mathbf{d}_{s,k_s,k_s} + b_{s,k_s,k_s} \right|^2 - \Gamma_{s,k_s} \left(\sum_{\substack{j \in \mathcal{K}_s \\ j \neq k_s}} \left| \boldsymbol{\theta}_s^T \mathbf{d}_{s,k_s,j} + b_{s,k_s,j} \right|^2 + \sigma^2 \right) \geq 0. \quad (14)$$

Then, the optimization problem for ϕ_s is formulated to maximize the sum of the left-hand side of (14) as

$$\max_{\phi_s} \sum_{k_s \in \mathcal{K}_s} \left(\left| \boldsymbol{\theta}_s^T \mathbf{d}_{s,k_s,k_s} + b_{s,k_s,k_s} \right|^2 - \Gamma_{s,k_s} \sum_{\substack{j \in \mathcal{K}_s \\ j \neq k_s}} \left| \boldsymbol{\theta}_s^T \mathbf{d}_{s,k_s,j} + b_{s,k_s,j} \right|^2 \right) \quad (15a)$$

$$\text{s.t. } \boldsymbol{\theta}_s = \exp(j\phi_s \odot \tilde{\mathbf{a}}_s), \quad (15b)$$

$$\phi_{s,m} \in (0, 2\pi], \quad \forall m. \quad (15c)$$

Different from the IRS reflection designs with the ideal reflection model, we notice that the practical reflection coefficient $\theta_{s,m}$ is determined by both the ideal phase-shift $\phi_{s,m}$ and the service selection indicator $a_{s,m}$ in constraint (15b). Particularly, when $a_{s,m} = 0$, $\theta_{s,m}$ is fixed as 1 regardless of the value $\phi_{s,m}$, i.e., optimizing $\phi_{s,m}$ cannot influence the objective value (15a). Therefore, we only need to optimize the phase-shift vector of the selected reflecting elements. Following this analysis, we divide the set of reflecting elements \mathcal{M} into the set of selected reflecting elements $\mathcal{I}_s \triangleq \{m | a_{s,m} = 1\}$ and the set of others $\mathcal{E}_s \triangleq \{m | a_{s,m} = 0\}$, and then correspondingly partition the phase-shift vector ϕ_s into $\widehat{\phi}_s$ which contains $\phi_{s,m}, \forall m \in \mathcal{I}_s$ and $\overline{\phi}_s$ which consists of $\phi_{s,m}, \forall m \in \mathcal{E}_s$, the practical reflection $\boldsymbol{\theta}_s$ into $\widehat{\boldsymbol{\theta}}_s$ and $\overline{\boldsymbol{\theta}}_s$, and $\mathbf{d}_{s,k_s,j}$ into $\widehat{\mathbf{d}}_{s,k_s,j}$ and $\overline{\mathbf{d}}_{s,k_s,j}$. It is obvious that $\widehat{\phi}_s$ is the required optimization variable, $\overline{\boldsymbol{\theta}}_s = \mathbf{1}$ and constraint (15b) is converted to $\widehat{\boldsymbol{\theta}}_s = \exp(j\widehat{\phi}_s)$. Thus, $\widehat{\phi}_s$ can be obtained by taking the angle of $\widehat{\boldsymbol{\theta}}_s$, and problem (15) with respect to $\widehat{\boldsymbol{\theta}}_s$ can be reformulated as

$$\min_{\widehat{\boldsymbol{\theta}}_s} - \widehat{\boldsymbol{\theta}}_s^T \mathbf{D}_s \widehat{\boldsymbol{\theta}}_s^* - \widehat{\boldsymbol{\theta}}_s^T \mathbf{b}_s - \mathbf{b}_s^H \widehat{\boldsymbol{\theta}}_s \quad (16a)$$

$$\text{s.t. } |\widehat{\theta}_{s,m}| = 1, \quad m = 1, \dots, |\mathcal{I}_s|, \quad (16b)$$

where \mathbf{D}_s and \mathbf{b}_s are defined in (12) as shown at the top of this page.

It can be observed that the main difficulty to tackle problem (16) is the non-convex unit modulus constraint (16b). In the literature of IRS optimization, non-convex relaxation, e.g., SDP/SDR, MM, and alternating minimization methods are usually exploited to handle constraint (16b) on the Euclidean space. However, a fast convergence and satisfactory performance cannot be guaranteed since either the objective function or the constraint is relaxed using these methods. Therefore, we propose to solve problem (16) on the Riemannian space. Specifically, the unit modulus constraint (16b) forms a smooth Riemannian manifold, on which problem (16) becomes an unconstrained problem. Since the Riemannian manifold resembles a Euclidean space at each point, lots of classic algorithms developed on the Euclidean space, e.g., steepest descent, conjugate gradient, quasi-Newton methods, have found their counterparts on the Riemannian manifold [45], [46]. In addition, since the objective function (16a) is a typical quadratic function with respect to $\widehat{\boldsymbol{\theta}}_s$, the required first-order and second-order derivatives in the above methods can be easily calculated as $-2\mathbf{D}_s \widehat{\boldsymbol{\theta}}_s^* - 2\mathbf{b}_s^H$ and $-2\mathbf{D}_s$, respectively. Therefore, problem (16) can be readily solved using the advanced Riemannian manifold based algorithms. Due to space limitations, the details are omitted in this paper.

After obtaining the solution $\widehat{\boldsymbol{\theta}}_s^*$ of problem (16), the ideal phase-shift $\phi_{s,m}^*, \forall m$, is updated by

$$\phi_{s,m}^* = \begin{cases} \angle \widehat{\theta}_{s,m}^*, & a_{s,m} = 1, \\ \phi_{s,m}, & a_{s,m} = 0. \end{cases} \quad (17)$$

B. Service Selection Design

With obtained transmit beamforming \mathbf{W}_s and ideal phase-shift vector ϕ_s for each BS, the original problem (9) is transformed into a service selection design problem. Since the service selection matrix \mathbf{A} cannot directly affect (9a), we should formulate another optimization problem to achieve better QoS for all users excepting to provide a larger feasible area, which can assist the joint transmit beamforming and practical phase-shift design in the next stage. Thus, similar to problem (15), the optimization problem for updating \mathbf{A} is formulated as

$$\max_{\mathbf{A}} \sum_{s \in \mathcal{S}} \sum_{k_s \in \mathcal{K}_s} \left(\left| \boldsymbol{\theta}_s^T \mathbf{d}_{s,k_s,k_s} + b_{s,k_s,k_s} \right|^2 - \Gamma_{s,k_s} \sum_{\substack{j \in \mathcal{K}_s \\ j \neq k_s}} \left| \boldsymbol{\theta}_s^T \mathbf{d}_{s,k_s,j} + b_{s,k_s,j} \right|^2 \right) \quad (18a)$$

$$\text{s.t. } \boldsymbol{\theta}_s = \exp(j\phi_s \odot \tilde{\mathbf{a}}_s), \quad \forall s, \quad (18b)$$

$$\|\mathbf{a}_m\|_0 \leq 1, \quad \forall m, \quad (18c)$$

$$a_{s,m} \in \{0, 1\}, \quad \forall s, m. \quad (18d)$$

Algorithm 1 Joint Transmit Beamforming and Practical IRS Reflection Design for Power Minimization Problem

Input: $\mathbf{h}_{\Gamma_s, k_s}^H$, \mathbf{G}_s , $\mathbf{h}_{\mathbf{d}_{s, k_s, j}}^H$, Γ_{s, k_s} , $\forall s \in \mathcal{S}, \forall k_s \in \mathcal{K}_s, \sigma^2$.

Output: \mathbf{W}_s^* , ϕ_s^* , $\forall s \in \mathcal{S}$, \mathbf{A}^* .

- 1: Initialize $\mathbf{A} = \mathbf{1}, \Phi$.
 - 2: **for** $s = 1$ to S **do**
 - 3: **while** no convergence for (10a) **do**
 - 4: Calculate \mathbf{W}_s^* by solving (11) with CVX.
 - 5: Obtain $\hat{\boldsymbol{\theta}}_s^*$ by solving (16) with Riemannian manifold optimizations.
 - 6: Construct ideal phase-shift ϕ_s^* by (17).
 - 7: **end while**
 - 8: **end for**
 - 9: **while** no convergence for \mathbf{A} **do**
 - 10: Obtain \mathbf{A} by solving (27).
 - 11: **end while**
 - 12: Repeat steps 2-8.
 - 13: Return $\mathbf{W}_s^*, \phi_s^*, \forall s \in \mathcal{S}, \mathbf{A}^* = [\mathbf{a}_1^*, \dots, \mathbf{a}_M^*]$.
-

Since the objective function is implicit with the variable \mathbf{A} , we first re-write it by substituting the equality constraint (18b) into (18a). Thus, the term $\boldsymbol{\theta}_s^T \mathbf{d}_{s, k_s, j} + b_{s, k_s, j}$ in (18a) can be equivalently re-written as

$$\begin{aligned} & \boldsymbol{\theta}_s^T \mathbf{d}_{s, k_s, j} + b_{s, k_s, j} \\ &= (\tilde{\mathbf{a}}_s^T \odot e^{j\phi_s^T}) \mathbf{d}_{s, k_s, j} + (\mathbf{1} - \tilde{\mathbf{a}}_s)^T \mathbf{d}_{s, k_s, j} + b_{s, k_s, j} \quad (19a) \\ &= \tilde{\mathbf{a}}_s^T \text{diag}\{e^{j\phi_s} - \mathbf{1}\} \mathbf{d}_{s, k_s, j} + \mathbf{1}^T \mathbf{d}_{s, k_s, j} + b_{s, k_s, j} \quad (19b) \\ &= \tilde{\mathbf{a}}_s^T \tilde{\mathbf{d}}_{s, k_s, j} + \tilde{b}_{s, k_s, j}, \quad (19c) \end{aligned}$$

where for simplicity we define

$$\tilde{\mathbf{d}}_{s, k_s, j} \triangleq \text{diag}\{e^{j\phi_s} - \mathbf{1}\} \mathbf{d}_{s, k_s, j}, \quad \forall s, k_s, j, \quad (20a)$$

$$\tilde{b}_{s, k_s, j} \triangleq \mathbf{1}^T \mathbf{d}_{s, k_s, j} + b_{s, k_s, j}, \quad \forall s, k_s, j. \quad (20b)$$

Then, by plugging (19c) into the objective (18a), expanding the quadratic terms, and ignoring the constant terms, the original problem (18) can be equivalently re-formulated as

$$\max_{\mathbf{A}} \sum_{s \in \mathcal{S}} \tilde{\mathbf{a}}_s^T \tilde{\mathbf{E}}_s \tilde{\mathbf{a}}_s - \sum_{s \in \mathcal{S}} \tilde{\mathbf{a}}_s^T \tilde{\mathbf{D}}_s \tilde{\mathbf{a}}_s + \sum_{s \in \mathcal{S}} \Re\{\tilde{\mathbf{a}}_s^T \tilde{\boldsymbol{\beta}}_s\} \quad (21a)$$

$$\text{s.t. } \|\mathbf{a}_m\|_0 \leq 1, \quad \forall m, \quad (21b)$$

$$a_{s, m} \in \{0, 1\}, \quad \forall s, m, \quad (21c)$$

where we define

$$\tilde{\mathbf{E}}_s \triangleq \sum_{k_s \in \mathcal{K}_s} (1 + \Gamma_{s, k_s}) \mathbf{d}_{s, k_s, j=k_s} \mathbf{d}_{s, k_s, j=k_s}^H, \quad \forall s, \quad (22a)$$

$$\tilde{\mathbf{D}}_s \triangleq \sum_{k_s \in \mathcal{K}_s} \Gamma_{s, k_s} \sum_{j \in \mathcal{K}_s} \mathbf{d}_{s, k_s, j} \mathbf{d}_{s, k_s, j}^H, \quad \forall s, \quad (22b)$$

$$\begin{aligned} \tilde{\boldsymbol{\beta}}_s \triangleq & 2 \sum_{k_s \in \mathcal{K}_s} (\mathbf{d}_{s, k_s, j=k_s} b_{s, k_s, j=k_s}^* \\ & - \Gamma_{s, k_s} \sum_{j \neq k_s} \mathbf{d}_{s, k_s, j} b_{s, k_s, j}^*), \quad \forall s. \quad (22c) \end{aligned}$$

It can be observed that problem (21) cannot be directly solved due to the non-convex objective function (21a) and the non-smooth constraints (21b) and (21c). Therefore, we propose to transform both the constraints and the objective function into more tractable forms in the followings.

Considering that each element of \mathbf{A} is binary as shown in constraint (21c), the 0-norm constraint (21b) can be equivalently transformed into a 1-norm constraint and re-formulated as:

$$\|\mathbf{a}_m\|_0 = \|\mathbf{a}_m\|_1 = \mathbf{1}^T \mathbf{a}_m \leq 1, \quad \forall m. \quad (23)$$

Then, by utilizing the difference-of-convex function method in [47], the binary constraint (21c) is transformed into:

$$0 \leq a_{s, m} \leq 1, \quad \forall s, m, \quad (24a)$$

$$\sum_{s \in \mathcal{S}} (\mathbf{1}^T \tilde{\mathbf{a}}_s - \tilde{\mathbf{a}}_s^T \tilde{\mathbf{a}}_s) \leq 0. \quad (24b)$$

Since the constraint (24b) is non-convex, we further apply the penalty method to move it to the objective and re-formulate the optimization problem as

$$\begin{aligned} \max_{\mathbf{A}} \sum_{s \in \mathcal{S}} \tilde{\mathbf{a}}_s^T \tilde{\mathbf{E}}_s \tilde{\mathbf{a}}_s - \sum_{s \in \mathcal{S}} \tilde{\mathbf{a}}_s^T \tilde{\mathbf{D}}_s \tilde{\mathbf{a}}_s + \sum_{s \in \mathcal{S}} \Re\{\tilde{\mathbf{a}}_s^T \tilde{\boldsymbol{\beta}}_s\} \\ - \tau \sum_{s \in \mathcal{S}} (\mathbf{1}^T \tilde{\mathbf{a}}_s - \tilde{\mathbf{a}}_s^T \tilde{\mathbf{a}}_s) \quad (25a) \end{aligned}$$

$$\text{s.t. } \mathbf{1}^T \mathbf{a}_m \leq 1, \quad \forall m, \quad (25b)$$

$$0 \leq a_{s, m} \leq 1, \quad \forall s, m, \quad (25c)$$

where $\tau > 0$ is a penalty factor. It is proved in [48] that the transform is equivalent when τ has a moderately high value. After obtaining the preferable linear constraints (25b) and (25c), the non-convex objective function (25a) is the major obstacle. In order to efficiently solve this problem, we employ the MM method and seek for a linear surrogate function of (25a) by utilizing the first-order Taylor expansion. Specifically, a lower-bounded surrogate function of the first term and last term in (25a) in the t -th iteration is derived as

$$\sum_{s \in \mathcal{S}} \tilde{\mathbf{a}}_s^T \tilde{\mathbf{E}}_s \tilde{\mathbf{a}}_s - \tau \sum_{s \in \mathcal{S}} (\mathbf{1}^T \tilde{\mathbf{a}}_s - \tilde{\mathbf{a}}_s^T \tilde{\mathbf{a}}_s) \quad (26a)$$

$$\begin{aligned} & \geq \sum_{s \in \mathcal{S}} [(\tilde{\mathbf{a}}_s^t)^T \tilde{\mathbf{E}}_s \tilde{\mathbf{a}}_s^t + 2\Re\{(\tilde{\mathbf{a}}_s - \tilde{\mathbf{a}}_s^t)^T \tilde{\mathbf{E}}_s \tilde{\mathbf{a}}_s^t\}] \\ & - \tau \sum_{s \in \mathcal{S}} [\mathbf{1}^T \tilde{\mathbf{a}}_s - (\tilde{\mathbf{a}}_s^t)^T \tilde{\mathbf{a}}_s^t - 2(\tilde{\mathbf{a}}_s^t)^T (\tilde{\mathbf{a}}_s - \tilde{\mathbf{a}}_s^t)], \quad (26b) \end{aligned}$$

where the vector $\tilde{\mathbf{a}}_s^t$ denotes the solution of the last iteration.

Based on the above derivations, by substituting the surrogate function (26b) into (25a), the optimization problem in the t -th iteration can be formulated as

$$\max_{\mathbf{A}} - \sum_{s \in \mathcal{S}} \tilde{\mathbf{a}}_s^T \tilde{\mathbf{D}}_s \tilde{\mathbf{a}}_s + \sum_{s \in \mathcal{S}} \Re\{\tilde{\mathbf{a}}_s^T \tilde{\boldsymbol{\beta}}_s\} + c \quad (27a)$$

$$\text{s.t. } \mathbf{1}^T \mathbf{a}_m \leq 1, \quad \forall m, \quad (27b)$$

$$0 \leq a_{s, m} \leq 1, \quad \forall s, m. \quad (27c)$$

where

$$\boldsymbol{\beta}_s \triangleq 2\tilde{\mathbf{E}}_s \tilde{\mathbf{a}}_s^t + \tau \tilde{\mathbf{a}}_s^t + \tilde{\boldsymbol{\beta}}_s, \quad \forall s, \quad (28a)$$

$$\begin{aligned} c \triangleq & \sum_{s \in \mathcal{S}} [(\tilde{\mathbf{a}}_s^t)^T \tilde{\mathbf{E}}_s \tilde{\mathbf{a}}_s^t - 2\Re\{(\tilde{\mathbf{a}}_s^t)^T \tilde{\mathbf{E}}_s \tilde{\mathbf{a}}_s^t\} \\ & - (\tilde{\mathbf{a}}_s^t)^T \lambda_s \tilde{\mathbf{a}}_s^t - \tau (\tilde{\mathbf{a}}_s^t)^T \tilde{\mathbf{a}}_s^t]. \quad (28b) \end{aligned}$$

It is obvious that problem (27) is a convex problem that can be efficiently solved by various existing methods.

C. Summary and Complexity Analysis

Summary: Based on the above derivations, the joint transmit beamforming and IRS reflection design for the power minimization problem (9) is straightforward and summarized in Algorithm 1. Given initialization $\mathbf{A} = \mathbf{1}$, the transmit beamforming and ideal phase-shifts for each BS are iteratively updated. Note that the reformulated objective function (13) is utilized in the iteration, theoretical convergence analysis cannot be easily obtained. But the simulation results shown in Sec. V illustrate that the proposed algorithm will converge fast to a local optimum. Then, the service selection matrix \mathbf{A}^* is optimized based on the obtained transmit beamforming and ideal phase-shift results. Finally, \mathbf{W}_s^* and ϕ_s^* are solved one more time with the obtained service selection matrix \mathbf{A}^* .

Complexity analysis: In each iteration, updating the transmit beamforming \mathbf{W}_s for each BS by solving a SOCP problem has a complexity of $\mathcal{O}(N_t^{4.5} K_s^{3.5})$; updating the ideal phase-shift vector $\hat{\boldsymbol{\theta}}_s$ using Riemannian manifold optimizations has a complexity of $\mathcal{O}(M^{1.5})$ at most. The complexity for updating the service selection matrix \mathbf{A} is $\mathcal{O}((SM)^3)$. Therefore, the total complexity of the proposed algorithm is of order $\mathcal{O}\{\sum_{s=1}^S (2N_t^{4.5} K_s^{3.5} + 2M^{1.5}) + (SM)^3\}$.

IV. ALGORITHMS FOR SUM-RATE MAXIMIZATION PROBLEM

In this section, we investigate the sum-rate maximization problem in the considered multi-cell multi-band systems. It is worth noting that the power minimization problem and the sum-rate maximization problem cannot be directly converted from one to another. In order to effectively handle this non-convex NP-hard optimization problem, the WMMSE approach and BCD method are employed to iteratively solve for each variable with a closed-form solution.

Specifically, our goal is to jointly optimize the transmit beamformers \mathbf{W} for the users of all BSs, the ideal IRS phase-shifts Φ , and the service selection matrix \mathbf{A} to maximize the sum-rate, subject to the transmit power budget of each BS and the practical IRS reflection model. Therefore, the optimization problem is formulated as

$$\max_{\mathbf{W}, \Phi, \mathbf{A}} \sum_{s \in \mathcal{S}} \sum_{k_s \in \mathcal{K}_s} \log_2(1 + \gamma_{s,k_s}) \quad (29a)$$

$$\text{s.t.} \quad \sum_{k_s \in \mathcal{K}_s} \|\mathbf{w}_{s,k_s}\|^2 \leq P_s, \quad \forall s, \quad (29b)$$

$$\boldsymbol{\theta}_s = \exp(j\phi_s \odot \tilde{\mathbf{a}}_s), \quad \forall s, \quad (29c)$$

$$\phi_{s,m} \in (0, 2\pi], \quad \forall s, m, \quad (29d)$$

$$\|\mathbf{a}_m\|_0 \leq 1, \quad a_{s,m} \in \{0, 1\}, \quad \forall s, m, \quad (29e)$$

where $P_s > 0$ denotes the transmit power budget of the s -th BS. Seeking for the solution to this non-convex NP-hard problem is very difficult, not only due to the complicated objective function (29a) that contains the fractional terms in $\log(\cdot)$, but also because of the coupled variables in the objective function (29a) and constraints (29c). Therefore, in the followings we first employ the WMMSE approach to convert the original optimization problem (29) into a more

tractable multi-variate problem and then use the BCD method to iteratively solve for each variable.

Although the WMMSE approach has been widely used for solving the sum-rate maximization problem, we would like to emphasize that the IRS beamforming design with the practical reflection model will be quite different and difficult due to the complicated constraint of each phase-shift element. Therefore, we need to develop an efficient algorithm to solve this sum-rate maximization problem (29), which for the first time considers the frequency-selective characteristic of the IRS in multi-cell networks.

A. Problem Reformulation by WMMSE

Following the derivations in [49], a scalar $\nu_{s,k_s} \in \mathbb{C}$ is applied for the k_s -th user to estimate the transmitted signal z_{s,k_s} . Then, the MSE of the k_s -th user can be calculated as

$$\begin{aligned} \text{MSE}_{s,k_s} &= \mathbb{E}\{(\nu_{s,k_s}^* y_{s,k_s} - z_{s,k_s})(\nu_{s,k_s}^* y_{s,k_s} - z_{s,k_s})^*\} \\ &= \sum_{j \in \mathcal{K}_s} |\nu_{s,k_s}^* (\mathbf{h}_{r,s,k_s}^H \boldsymbol{\Theta}_s \mathbf{G}_s + \mathbf{h}_{d,s,k_s}^H) \mathbf{w}_{s,j}|^2 \\ &\quad - 2\Re\{\nu_{s,k_s}^* (\mathbf{h}_{r,s,k_s}^H \boldsymbol{\Theta}_s \mathbf{G}_s + \mathbf{h}_{d,s,k_s}^H) \mathbf{w}_{s,k_s}\} \\ &\quad + |\nu_{s,k_s}|^2 \sigma^2 + 1, \quad \forall s, k_s. \end{aligned} \quad (30)$$

Introducing the MSE weights $\mu_{s,k_s} \in \mathbb{R}^+$, $\forall s, k_s$, the sum-rate maximization problem (29) is equivalently reformulated as:

$$\min_{\mathbf{W}, \Phi, \mathbf{A}, \boldsymbol{\nu}, \boldsymbol{\mu}} \sum_{s \in \mathcal{S}} \sum_{k_s \in \mathcal{K}_s} (\mu_{s,k_s} \text{MSE}_{s,k_s} - \log_2 \mu_{s,k_s}) \quad (31a)$$

$$\text{s.t.} \quad (29b) - (29e), \quad (31b)$$

where $\boldsymbol{\mu}$ and $\boldsymbol{\nu}$ denote the vectors that contain the auxiliary variables μ_{s,k_s} and ν_{s,k_s} , $\forall s, k_s$, respectively. Since the complicated $\log_2(1 + \gamma_{s,k_s})$ term in the objective function is transformed into a polynomial term and a very simple $\log_2(\cdot)$ term, the reformulated optimization problem (31) is much more tractable. Specifically, the obtained multi-variate optimization problem (31) can be solved using the typical BCD method. The details for updating each variable are presented in the next subsection.

B. Block Update by BCD

1) *Update $\boldsymbol{\nu}$:* With given the transmit beamformer \mathbf{W} , the ideal IRS phase-shift Φ , the service selection matrix \mathbf{A} , and the MSE weight vector $\boldsymbol{\mu}$, the design of $\boldsymbol{\nu}$ for each user is independent. The optimization problem of solving for ν_{s,k_s} can be expressed as

$$\begin{aligned} \min_{\nu_{s,k_s}} & |\nu_{s,k_s}|^2 \left(\sum_{j \in \mathcal{K}_s} |(\mathbf{h}_{r,s,k_s}^H \boldsymbol{\Theta}_s \mathbf{G}_s + \mathbf{h}_{d,s,k_s}^H) \mathbf{w}_{s,j}|^2 + \sigma^2 \right) \\ & - 2\Re\{\nu_{s,k_s}^* (\mathbf{h}_{r,s,k_s}^H \boldsymbol{\Theta}_s \mathbf{G}_s + \mathbf{h}_{d,s,k_s}^H) \mathbf{w}_{s,k_s}\}, \end{aligned} \quad (32)$$

which is an unconstrained quadratic convex problem. Thus, setting the first-order derivative with respect to ν_{s,k_s} to zero, the optimal solution ν_{s,k_s}^* can be easily calculated as

$$\nu_{s,k_s}^* = \frac{(\mathbf{h}_{r,s,k_s}^H \boldsymbol{\Theta}_s \mathbf{G}_s + \mathbf{h}_{d,s,k_s}^H) \mathbf{w}_{s,k_s}}{\sum_{j \in \mathcal{K}_s} |(\mathbf{h}_{r,s,k_s}^H \boldsymbol{\Theta}_s \mathbf{G}_s + \mathbf{h}_{d,s,k_s}^H) \mathbf{w}_{s,j}|^2 + \sigma^2}. \quad (33)$$

$$\mathbf{B}_s \triangleq \sum_{k_s \in \mathcal{K}_s} \mu_{s,k_s} |\nu_{s,k_s}|^2 \text{diag}\{\mathbf{h}_{r,s,k_s}^H\} \mathbf{G}_s \sum_{j \in \mathcal{K}_s} \mathbf{w}_{s,j} \mathbf{w}_{s,j}^H \mathbf{G}_s^H \text{diag}\{\mathbf{h}_{r,s,k_s}\}, \forall s, \quad (34a)$$

$$\mathbf{c}_s \triangleq \sum_{k_s \in \mathcal{K}_s} \mu_{s,k_s} \nu_{s,k_s}^* \text{diag}\{\mathbf{h}_{r,s,k_s}^H\} \mathbf{G}_s \mathbf{w}_{s,k_s} \left(1 - \nu_{s,k_s} \sum_{j \in \mathcal{K}_s} \mathbf{w}_{s,j} \mathbf{w}_{s,j}^H \mathbf{h}_{d,s,k_s}\right), \forall s. \quad (34b)$$

2) *Update μ* : Fixing the transmit beamformer \mathbf{W} , the ideal IRS phase-shift Φ , the service selection matrix \mathbf{A} , and the variable ν , the optimization problem with respect to each independent MSE weight μ_{s,k_s} can be formulated as

$$\min_{\mu_{s,k_s}} \mu_{s,k_s} \text{MSE}_{s,k_s} - \log_2 \mu_{s,k_s}. \quad (35)$$

Similarly, the optimal solution μ_{s,k_s}^* can be obtained by applying the typical first-order optimality condition as

$$\mu_{s,k_s}^* = \text{MSE}_{s,k_s}^{-1} \stackrel{(a)}{=} 1 + \gamma_{s,k_s}, \quad (36)$$

where (a) is derived by substituting the optimal ν_{s,k_s}^* in (33) into MSE_{s,k_s} in (30).

3) *Update \mathbf{W}* : After obtaining the variable ν , the MSE weight μ , the ideal IRS phase-shift Φ , and the service selection matrix \mathbf{A} , the optimization problem for designing the transmit beamformer \mathbf{W}_s for the s -th BS can be formulated as

$$\min_{\mathbf{W}_s} \sum_{k_s \in \mathcal{K}_s} \mu_{s,k_s} \left(\sum_{j \in \mathcal{K}_s} |\bar{\mathbf{h}}_{s,k_s}^H \mathbf{w}_{s,j}|^2 - 2\Re\{\bar{\mathbf{h}}_{s,k_s}^H \mathbf{w}_{s,k_s}\} \right) \quad (37a)$$

$$\text{s.t.} \quad \sum_{k_s \in \mathcal{K}_s} \|\mathbf{w}_{s,k_s}\|^2 \leq P_s, \quad (37b)$$

where we define $\bar{\mathbf{h}}_{s,k_s}^H \triangleq \nu_{s,k_s}^* (\mathbf{h}_{r,s,k_s}^H \Theta_s \mathbf{G}_s + \mathbf{h}_{d,s,k_s}^H)$ for brevity. Note that (37) is a convex optimization problem, which can be readily solved using standard convex optimization algorithms, e.g., the interior-point algorithm. In order to reduce the execution time, we employ the typical Lagrange multiplier method to obtain a closed-form solution. Attaching a Lagrange multiplier $\lambda_s \geq 0$ to the power constraint (37b), the Lagrange function of problem (37) can be formulated as

$$\begin{aligned} \mathcal{L}(\mathbf{W}_s, \lambda_s) &\triangleq \sum_{k_s \in \mathcal{K}_s} \mu_{s,k_s} \left(\sum_{j \in \mathcal{K}_s} |\bar{\mathbf{h}}_{s,k_s}^H \mathbf{w}_{s,j}|^2 - 2\Re\{\bar{\mathbf{h}}_{s,k_s}^H \mathbf{w}_{s,k_s}\} \right) \\ &\quad + \lambda_s \left(\sum_{k_s \in \mathcal{K}_s} \|\mathbf{w}_{s,k_s}\|^2 - P_s \right) \end{aligned} \quad (38a)$$

$$\begin{aligned} &= \sum_{k_s \in \mathcal{K}_s} \left(\mathbf{w}_{s,k_s}^H \sum_{j \in \mathcal{K}_s} \mu_{s,j} \bar{\mathbf{h}}_{s,j} \bar{\mathbf{h}}_{s,j}^H \mathbf{w}_{s,k_s} - 2\mu_{s,k_s} \Re\{\bar{\mathbf{h}}_{s,k_s}^H \mathbf{w}_{s,k_s}\} \right. \\ &\quad \left. + \lambda_s \mathbf{w}_{s,k_s}^H \mathbf{w}_{s,k_s} \right) - \lambda_s P_s. \end{aligned} \quad (38b)$$

Then, setting $\frac{\partial \mathcal{L}(\mathbf{W}_s, \lambda_s)}{\partial \mathbf{w}_{s,k_s}} = \mathbf{0}$, the optimal beamforming vector \mathbf{w}_{s,k_s}^* is given by

$$\mathbf{w}_{s,k_s}^* = \mu_{s,k_s} \left(\sum_{j \in \mathcal{K}_s} \mu_{s,j} \bar{\mathbf{h}}_{s,j} \bar{\mathbf{h}}_{s,j}^H + \lambda_s \mathbf{I}_{N_t} \right)^{-1} \bar{\mathbf{h}}_{s,k_s}, \quad (39)$$

where the Lagrange multiplier $\lambda_s \geq 0$ should be guaranteed to satisfy the complementarity slackness condition of the power

constraint (37b). Plugging the obtained transmit beamformers \mathbf{w}_{s,k_s}^* , $\forall k_s$, into the power constraint (37b), the optimal solution of λ_s can be easily obtained by one dimensional search methods, e.g., the bisection search method.

4) *Update Φ and \mathbf{A}* : Since the ideal IRS phase-shift Φ is closely associated with the service selection \mathbf{A} in designing the practical IRS reflection Θ for all BSs, a joint design for Φ and \mathbf{A} is necessary to achieve a satisfactory performance, which has not been considered in the existing literature. Thus, with the fixed variable ν , MSE weight μ , and transmit beamformer \mathbf{W} , the optimization problem for the joint ideal IRS phase-shift Φ and service selection matrix \mathbf{A} design is written by

$$\min_{\Phi, \mathbf{A}} \sum_{s \in \mathcal{S}} \sum_{k_s \in \mathcal{K}_s} \mu_{s,k_s} \left[\sum_{j \in \mathcal{K}_s} |\nu_{s,k_s}^* (\mathbf{h}_{r,s,k_s}^H \Theta_s \mathbf{G}_s + \mathbf{h}_{d,s,k_s}^H) \mathbf{w}_{s,j}|^2 - 2\Re\{\nu_{s,k_s}^* (\mathbf{h}_{r,s,k_s}^H \Theta_s \mathbf{G}_s + \mathbf{h}_{d,s,k_s}^H) \mathbf{w}_{s,k_s}\} \right] \quad (40a)$$

$$\text{s.t.} \quad (29c) - (29e). \quad (40b)$$

For brevity, we define \mathbf{B}_s and \mathbf{c}_s , which are presented in (34) on the top of this page, and rearrange problem (40) as

$$\min_{\Phi, \mathbf{A}} \sum_{s=1}^S \left(\theta_s^H \mathbf{B}_s \theta_s - 2\Re\{\theta_s^H \mathbf{c}_s\} \right) \quad (41a)$$

$$\text{s.t.} \quad \theta_s = \exp(j\phi_s \odot \tilde{\mathbf{a}}_s), \quad \forall s, \quad (41b)$$

$$\phi_{s,m} \in (0, 2\pi], \quad \forall s, m, \quad (41c)$$

$$\|\mathbf{a}_m\|_0 \leq 1, \quad a_{s,m} \in \{0, 1\}, \quad \forall s, m. \quad (41d)$$

Due to the joint optimization of the M reflecting elements and the non-convex constraint (41d) of each reflecting element, it is very difficult to directly seek for an optimal solution to problem (41). Therefore, we attempt to decompose problem (41) into M sub-problems, each of which jointly designs the ideal phase-shifts and service selection of a certain reflecting element with the other reflecting elements fixed. To this end, we first split the objective function (41a) as

$$\sum_{s=1}^S \left(\theta_s^H \mathbf{B}_s \theta_s - 2\Re\{\theta_s^H \mathbf{c}_s\} \right) \quad (42a)$$

$$\stackrel{(b)}{=} \sum_{s=1}^S \sum_{m=1}^M \left[\sum_{n=1}^M \mathbf{B}_s(m, n) \theta_{s,m}^* \theta_{s,n} - 2\Re\{\theta_{s,m}^* \mathbf{c}_s(m)\} \right] \quad (42b)$$

$$\stackrel{(c)}{=} \sum_{s=1}^S \left[\sum_{n \neq m} \left(\mathbf{B}_s(m, n) \theta_{s,m}^* \theta_{s,n} + \mathbf{B}_s(n, m) \theta_{s,n}^* \theta_{s,m} \right) + \mathbf{B}_s(m, m) |\theta_{s,m}|^2 - 2\Re\{\theta_{s,m}^* \mathbf{c}_s(m)\} \right], \quad (42c)$$

$$\stackrel{(d)}{=} \sum_{s=1}^S \left(2\Re\{\zeta_{s,m} \theta_{s,m}^*\} + \mathbf{B}_s(m, m) \right), \quad (42d)$$

Algorithm 2 Joint Transmit Beamforming and Practical IRS Reflection Design for Sum-Rate Maximization Problem

Input: \mathbf{h}_{r,s,k_s}^H , \mathbf{G}_s , \mathbf{h}_{d,s,k_s}^H , P_s , $\forall s \in \mathcal{S}$, $\forall k_s \in \mathcal{K}_s$, σ^2 .
Output: \mathbf{w}_{s,k_s}^* , $\forall s \in \mathcal{S}$, $\forall k_s \in \mathcal{K}_s$, ϕ_m^* , $\forall m \in \mathcal{M}$, \mathbf{A}^* .

- 1: Initialize \mathbf{A} , Φ , \mathbf{W} .
- 2: **while** no convergence of the objective (31a) **do**
- 3: Update ν_{s,k_s} , $\forall s \in \mathcal{S}$, $\forall k_s \in \mathcal{K}_s$ by (33).
- 4: Update μ_{s,k_s} , $\forall s \in \mathcal{S}$, $\forall k_s \in \mathcal{K}_s$ by (36).
- 5: Update \mathbf{w}_{s,k_s} , $\forall s \in \mathcal{S}$, $\forall k_s \in \mathcal{K}_s$ by (39).
- 6: **while** no convergence of the objective (41a) **do**
- 7: **for** $m = 1 : M$ **do**
- 8: Obtain s^* by solving (45).
- 9: Update $\phi_{s^*,m}$ by (44).
- 10: Update \mathbf{a}_m by (46).
- 11: **end for**
- 12: **end while**
- 13: **end while**
- 14: Return \mathbf{w}_{s,k_s}^* , $\forall s \in \mathcal{S}$, $\forall k_s \in \mathcal{K}_s$, ϕ_m^* , $\forall m \in \mathcal{M}$, $\mathbf{A}^* = [\mathbf{a}_1^*, \dots, \mathbf{a}_M^*]$.

where $\zeta_{s,m} \triangleq \sum_{m \neq n} \mathbf{B}_s(m,n) \theta_{s,n} - \mathbf{c}_s(m)$ for brevity. In particular, step (b) unfolds the quadratic term of θ_s , step (c) separates the reflection coefficients of the m -th reflecting elements and the others, and step (d) is derived based on $\mathbf{B}_s = \mathbf{B}_s^H$ and $|\theta_{s,m}| = 1$.

Based on the derivations in (42), when we only consider the m -th reflecting element, its corresponding ideal phase-shifts vector $\tilde{\phi}_m \triangleq [\phi_{1,m}, \dots, \phi_{S,m}]^T$ of all BSs and service selection vector \mathbf{a}_m are jointly designed. Thus, after discarding some constant and irrelevant terms, the m -th sub-problem is formulated as

$$\min_{\tilde{\phi}_m, \mathbf{a}_m} \sum_{s=1}^S |\zeta_{s,m}| \cos(\angle \zeta_{s,m} - \phi_{s,m} a_{s,m}) \quad (43a)$$

$$\text{s.t. } \phi_{s,m} \in (0, 2\pi], \forall s, \quad (43b)$$

$$\|\mathbf{a}_m\|_0 \leq 1, \quad a_{s,m} \in \{0, 1\}, \quad \forall s. \quad (43c)$$

We observe that the binary vector \mathbf{a}_m contains at most one non-zero entry according to constraint (43c). If $a_{s,m} = 0$, there is no need to optimize $\phi_{s,m}$ since it cannot change the objective value. Meanwhile, if $a_{s,m} = 1$, there must exist a $\phi_{s,m} = \pi + \angle \zeta_{s,m}$ that achieves the minimum value $-|\zeta_{s,m}|$ of the s -th term in (43a). Therefore, the optimal solution \mathbf{a}_m^* to problem (43) is a non-zero vector. We assume the s^* -th entry of \mathbf{a}_m^* is 1 and thus only the s^* -th entry of $\tilde{\phi}_m$ is updated by

$$\phi_{s^*,m} = \pi + \angle \zeta_{s^*,m}. \quad (44)$$

Then, the optimization problem (43) is converted into

$$\min_{s^*} \sum_{\substack{s=1 \\ s \neq s^*}}^S |\zeta_{s,m}| \cos \angle \zeta_{s,m} - |\zeta_{s^*,m}| \quad (45a)$$

$$\text{s.t. } s^* = 1, 2, \dots, S, \quad (45b)$$

which can be easily solved by exhaustively searching its feasible set (45b). After finding s^* , the optimal ideal phase-shift $\phi_{s^*,m}$ is updated by (44) and the optimal service selection vector \mathbf{a}_m^* is determined by

$$a_{s^*,m} = 1, \quad a_{s,m} = 0, \quad \forall s \in \mathcal{S}, s \neq s^*. \quad (46)$$

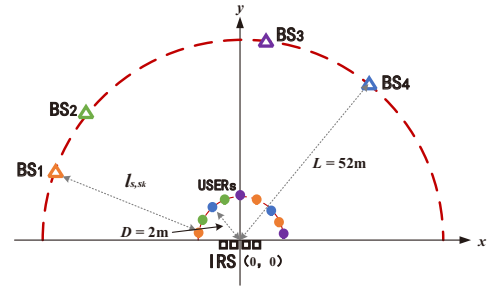


Fig. 4: An illustration of the relative position among the BSs, IRS, and users.

C. Summary and Complexity Analysis

Summary: Based on the above derivations, the joint transmit beamforming and practical IRS reflection design for sum-rate maximization problem is straightforward and summarized in Algorithm 2. With an appropriate initialization, the variable ν , the MSE weight μ , the transmit beamformer \mathbf{W} , and the practical IRS reflection $\Theta = \exp(\Phi \odot \mathbf{A})$, are iteratively updated until the convergence is met. Since the objective function value at each step is nondecreasing, we can guarantee that the BCD method can strictly converge to a local optimum point. In addition, in the initialization, the service selection matrix \mathbf{A} and the ideal phase-shift Φ are randomly generated from their corresponding feasible sets, and the transmit beamformer of each BS adopts the typical MMSE beamformer.

Complexity analysis: In each iteration, updating ν has a complexity of $\mathcal{O}\{\sum_{s \in \mathcal{S}} K_s(K_s + 1)N_t M^2\}$; updating μ has a complexity of $\mathcal{O}\{\sum_{s \in \mathcal{S}} K_s^2 N_t M^2\}$; updating transmit beamformer \mathbf{W} requires about $\mathcal{O}\{\sum_{s \in \mathcal{S}} N_t K_s(3M^2 + N_t^2)\}$ operations. Finally, the order of complexity for updating ideal IRS phase-shifts Φ and service selection matrix \mathbf{A} is about $\mathcal{O}\{\sum_{s \in \mathcal{S}} [(M-1)(K_s^3 M^2 N_t^2 + K_s^3 M N_t^2)]\}$. Therefore, the total complexity of the proposed algorithm is $\mathcal{O}\{\sum_{s \in \mathcal{S}} K_s [(2K_s + 1)N_t M^2 + K_s(3M^2 + N_t^2) + K_s^2(M N_t^2(M-1)(M+N_t))]\}$.

V. SIMULATION RESULTS

In this section, extensive simulation results are presented to demonstrate the significance of using the proposed practical IRS reflection model in the IRS-assisted multi-cell multi-band system and the effectiveness of our proposed algorithms. All simulations are implemented on a computer with Intel(R) Core(TM) i7-9700 CPU, NVIDIA GeForce GT-710 GPU, Matlab Version 2020b, CVX toolbox Version 2.2, and Manopt toolbox Version 7.0. We assume that the multi-cell multi-band system consists of $S = 3$ or $S = 4$ cells/BSs. In each cell, the BS equipped with $N_t = 16$ antennas serves $K = K_s = 3$, $\forall s$, single-antenna users. An IRS composed of $M = 64$ reflecting elements is deployed to assist the downlink communications for the considered system. The noise power is set as $\sigma^2 = -70$ dBm. The QoS requirement of each user and the power budget of each BS are the same, i.e., $\Gamma = \Gamma_{s,k_s} = 5$ dB, $\forall s, \forall k_s$, and $P = P_s = -5$ dB, $\forall s$. In

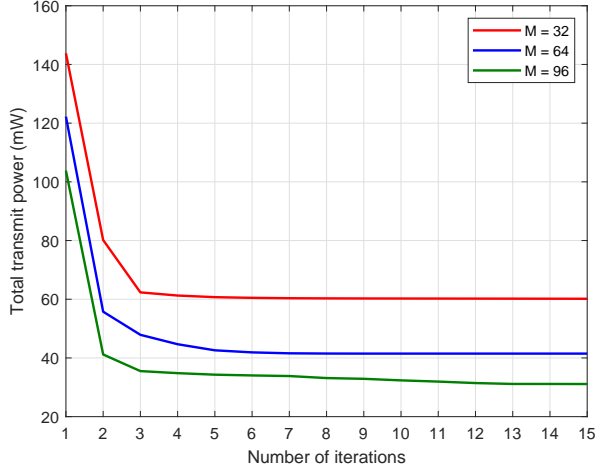


Fig. 5: Transmit power versus the number of iterations ($N_t = 16$, $S = 3$, $K = 3$, $\Gamma = 5\text{dB}$).

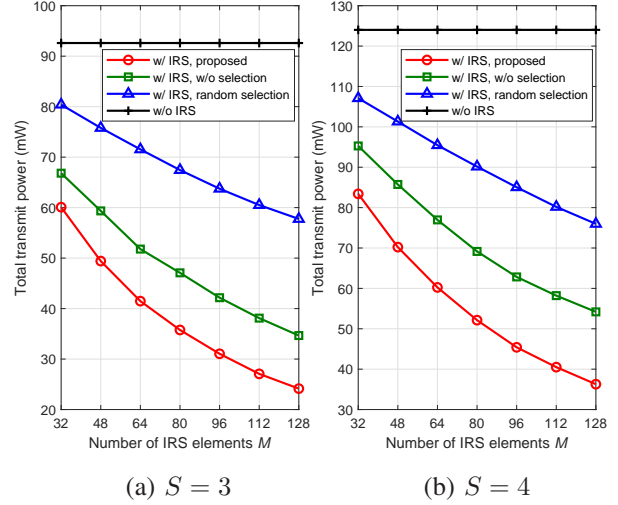


Fig. 7: Total transmit power versus the number of IRS reflecting elements M ($\Gamma = 5\text{dB}$, $N_t = 16$, $K = 3$).

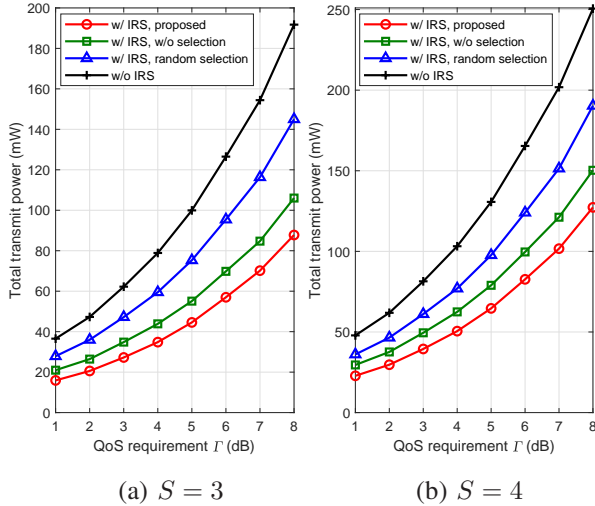


Fig. 6: Total transmit power versus the QoS requirement Γ ($M = 64$, $N_t = 16$, $K = 3$).

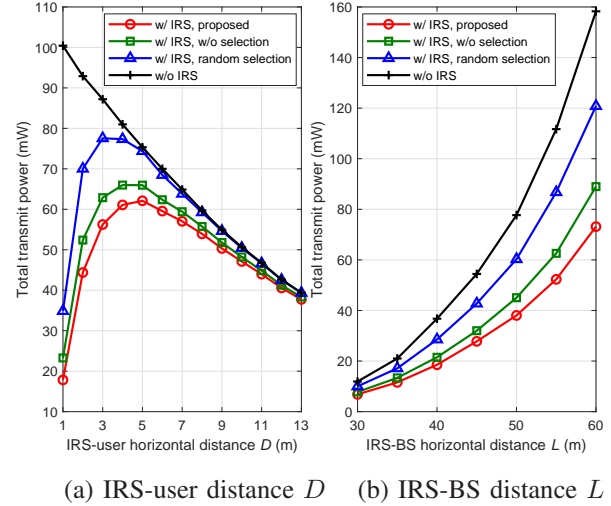


Fig. 8: Total transmit power versus the distance between BSs, IRS, and users ($M = 64$, $\Gamma = 5\text{dB}$, $N_t = 16$, $S = 3$, $K = 3$).

addition, the distance-dependent channel path loss³ is modeled as $\eta(d) = C_0(\frac{d}{d_0})^{-\alpha}$, where $C_0 = -30\text{dB}$ denotes the signal attenuation at the reference distance $d_0 = 1\text{m}$, and α denotes the path loss exponent. We set the path loss exponents for the BS-IRS, IRS-user, and BS-user channels as 2.5, 2.8, and 3.5, respectively.

A two-dimensional coordinate system is shown in Fig. 4 to demonstrate the position relationship of different devices in the considered systems from a top-down view. For both cases of $S = 3$ BSs and $S = 4$ BSs, the IRS is located at $(0, 0)$, and the BSs are randomly distributed at a distance of $L = 52\text{m}$ away from the IRS. Since the IRS is deployed to enhance the transmission quality for the edge users, we assume that the

users in each cell are randomly distributed $D = 2\text{m}$ away from the IRS.

A. Power Minimization Problem

In this subsection, we show the simulation results for the power minimization problem in Figs. 5-8. The transmit power versus the number of iterations is first presented in Fig. 5 to show the convergence of the proposed algorithm. It can be observed that the convergence can be met within 12 iterations under different settings and the scheme with lesser IRS reflecting elements has faster convergence due to the reduced dimension of variables. These convergence results support the low-complexity implementation.

Fig. 6 shows the total transmit power versus the QoS requirement Γ for the cases that $S = 3$ and $S = 4$. Our algorithm based on the proposed practical IRS reflection model in this paper is denoted as “w/ IRS, proposed”. The practical

³This assumption is widely used in the existing works [7], [14], [15], [20], [22]-[24], [26]-[30]. Moreover, proposed practical IRS reflection model and associated algorithms are also suitable for other realistic propagation environments in [50].

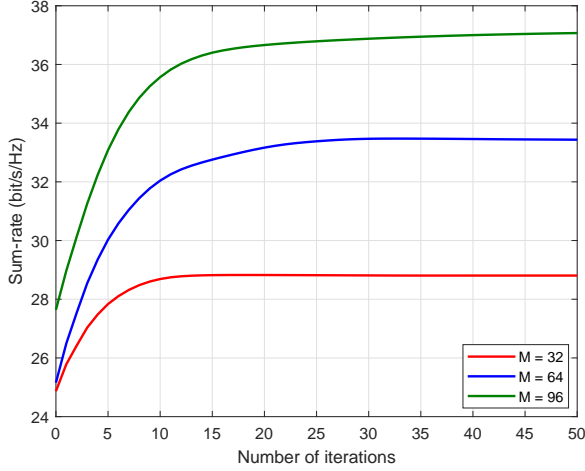
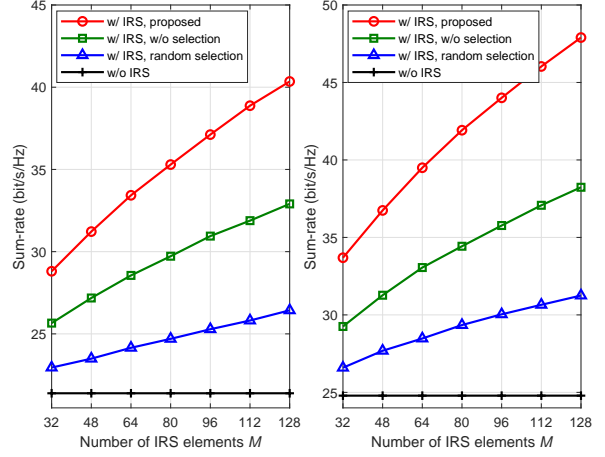


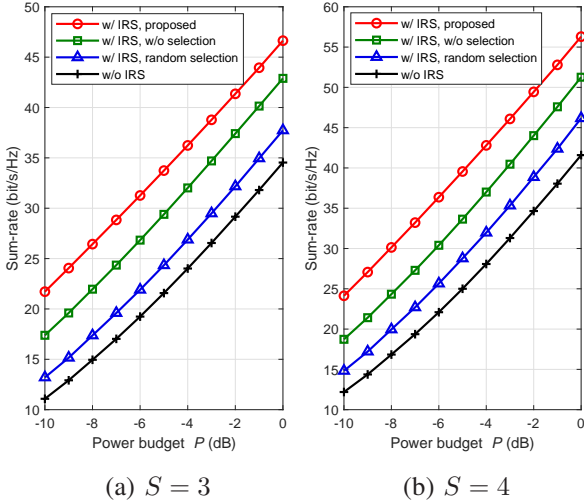
Fig. 9: Sum-rate versus the number of iterations ($P = -5\text{dB}$, $N_t = 16$, $S = 3$, $K = 3$).



(a) $S = 3$

(b) $S = 4$

Fig. 11: Sum-rate versus the number of IRS reflecting elements M ($P = -5\text{dB}$, $N_t = 16$, $K = 3$).

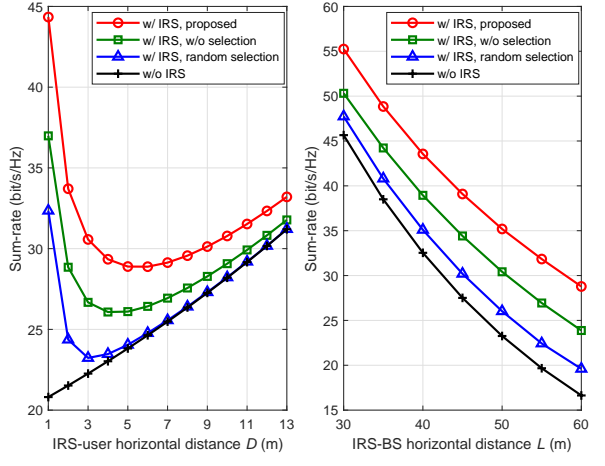


(a) $S = 3$

(b) $S = 4$

Fig. 10: Sum-rate versus the power budget P ($M = 64$, $N_t = 16$, $K = 3$).

IRS reflection model for the considered multi-cell multi-band systems exhibits that each reflecting element is independently selected to serve a certain BS. Therefore, for comparison we also include *i)* the scenario that all reflecting elements are selected to serve the same BS, i.e., the IRS provides tunable phase-shifts for a certain BS while exhibits fixed 0° phase-shifts for other BSs, which is denoted as “w/ IRS, w/o selection”; *ii)* the scheme that each reflecting element is randomly selected to serve a certain BS, which is denoted as “w/ IRS, random selection”; *iii)* the case without deploying the IRS, which is denoted as “w/o IRS”. We can easily observe from Fig. 6 that the proposed algorithm requires less transmit power than the “w/ IRS, random selection” and “w/o IRS” schemes for all transmit power ranges, which validates the advantages of deploying IRS in wireless communication systems. Moreover, the proposed algorithm outperforms the “w/ IRS, w/o selection” scheme, which verifies the importance of joint designing the transmit beamforming, ideal phase-shift



(a) IRS-user distance D

(b) IRS-BS distance L

Fig. 12: Sum-rate versus the distance between BSs, IRS, and users ($M = 64$, $P = -5\text{dB}$, $N_t = 16$, $S = 3$, $K = 3$).

design, and IRS service selection.

Then, the transmit power versus the number of IRS reflecting elements M is plotted in Fig. 7. A similar conclusion can be drawn as that from Fig. 6. We also observe that the transmit power of all schemes decreases with the increasing number of IRS reflecting elements, and the power reduction of our proposed algorithm is more remarkable, which validates the advancement of the proposed practical model and design algorithm in playing the role of the IRS.

To show the impact of IRS location, Fig. 8 illustrates the total transmit power as functions of the IRS-user distance D and IRS-BS distance L . It can be observed in Fig. 8 (a) that for the schemes with IRS, when the users move away from the IRS towards the BSs, the transmit power increases at first, because the reflected signals from the IRS becomes weaker, and then decreases thanks to stronger signals from BSs. It is worth noting that our proposed algorithm always has better performance and service coverage. For the “w/o IRS” scheme,

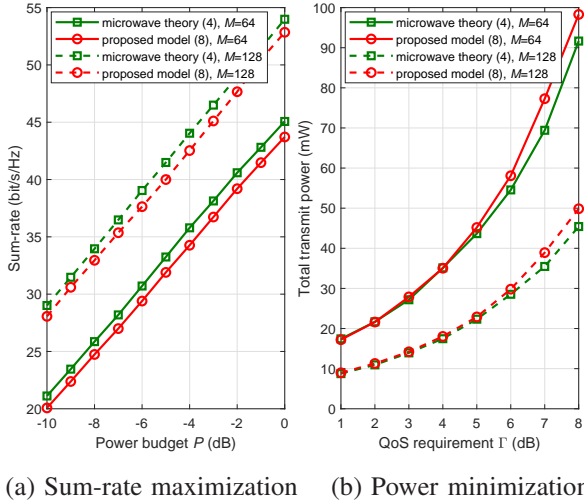


Fig. 13: Performance comparison between the practical response and the proposed model ($M = 64$, $N_t = 16$, $S = 3$, $K = 3$).

the transmit power keeps decreasing since the users move closer to their corresponding BSs. When users are randomly distributed at a distance of $D = 2\text{m}$ away from the IRS, the total transmit power versus the IRS-BS distance L is shown in Fig. 8 (b). The longer distance between BS and IRS, the more significant performance improvement of deploying IRS. Moreover, our proposed algorithm always outperforms the others under different IRS-user and IRS-BS distance settings.

B. Sum-rate Maximization Problem

In this subsection, the simulation results for the sum-rate maximization problem are demonstrated in Figs. 9-12. A similar fast convergence performance as that for the power minimization problem is also observed in Fig. 9.

Fig. 10 shows the sum-rate versus the power budget P for the scenarios that $S = 3$ and $S = 4$. It can be seen that more transmit power provides a larger sum-rate for all schemes and the proposed algorithm always significantly outperforms the others under different settings. Specifically, our proposed algorithm can provide about 3dB gain compared with the scheme without BS selection, and more than 4dB gain compared with the scheme with random BS selection. The sum-rate versus the number of IRS reflecting elements M is illustrated in Fig. 11. Similar conclusion can be drawn as that from Fig. 7. Note that our proposed algorithm has a larger performance improvement with the increase of M . This is because more reflecting elements can provide larger passive beamforming gain, while the practical model and proposed design algorithm can utilize all IRS elements more efficiently. The sum-rate versus the IRS-user distance D and IRS-BS distance L are presented in Fig. 12 (a) and (b), respectively. The impact of the IRS locations on the system performance is consistent with that in Fig. 8, which further demonstrates the importance of IRS deployment with the proposed design algorithm in practical systems.

C. Analysis of Model Errors

In order to illustrate the impact of the phase approximation of the proposed IRS model in Table. I on the degradation of system performance, Fig. 13 compares the performances using the microwave theory based actual response expressed in (4), and the proposed simplified model (8). Specifically, when the microwave theory (4) is used, the phase-shift response of other frequencies is not approximated as unchanged, but also varied accordingly. However, the microwave theory (4) is extremely complicated and no existing algorithm can be directly adopted. Thus, we iteratively design the IRS phase-shift for each element by one-dimensional exhaustive search with fixed other elements. As seen from Fig. 13, the microwave theory based actual response (4) can provide slightly better performance than our proposed simplified model. However, the exhaustive search algorithm that enables the design under complex nonlinear equation (4) causes significantly higher computational complexity. For example, for a 64-element IRS-assisted system, the beamforming design with the microwave theory (4) takes an average of 46.217 seconds using the exhaustive search method, while the proposed simplified model (8) only requires an average of 1.072 seconds using our proposed beamforming design algorithm. Therefore, we can conclude that our proposed model can facilitate the beamforming design with negligible performance loss.

VI. CONCLUSIONS

In this paper, we first derived a practical yet tractable IRS reflection model for an IRS-assisted multi-cell multi-band system. Based on the proposed model, we investigated the joint transmit beamforming and IRS reflection designs for both power minimization and sum-rate maximization problems. Efficient algorithms were proposed to solve them by exploiting SOCP, Riemannian manifold, WMMSE, BCD, and the proposed efficient search algorithms. Simulation results demonstrated significant performance improvement of the proposed algorithms, which confirmed the importance of using the proposed practical reflection model and the joint beamforming and IRS reflection designs in IRS-assisted multi-cell multi-band systems. Moreover, there are many issues of IRS-assisted systems with the practical reflection model worth being investigated in future works, including more sophisticated beamforming design algorithms, fast channel estimation, influence of CSI errors, as well as learning-based methods, etc.

REFERENCES

- [1] A. Gatherer, "What will 6G be?" Jun. 2018. [Online]. Available: <https://www.comsoc.org/publications/ctn/what-will-6g-be>
- [2] F. Boccardi, R. W. Heath, A. Lozano, T. L. Marzetta, and P. Popovski, "Five disruptive technology directions for 5G," *IEEE Commun. Mag.*, vol. 52, no. 2, pp. 74-80, Feb. 2014.
- [3] J. G. Andrews, S. Buzzi, W. Choi, S. V. Hanly, A. Lozano, A. C. K. Soong, and J. C. Zhang, "What will 5G be?" *IEEE J. Sel. Areas Commun.*, vol. 32, no. 6, pp. 1065-1082, Jun. 2014.
- [4] Q. Wu, S. Zhang, B. Xiong, C. You, and R. Zhang, "Intelligent reflecting surface aided wireless communications: A tutorial," *IEEE Trans. Commun.*, vol. 69, no. 5, pp. 3313-3351, Jan. 2021.
- [5] E. Basar, M. D. Renzo, J. Rosny, M. Debbah, M.-S. Alouini, and R. Zhang, "Wireless communications through reconfigurable intelligent surfaces," *IEEE Access*, vol. 7, pp. 116753-116773, Aug. 2019.

- [6] Q. Wu and R. Zhang, "Towards smart and reconfigurable environment: Intelligent reflecting surface aided wireless network," *IEEE Commun. Mag.*, vol. 58, no. 1, pp. 106-112, Jan. 2020.
- [7] S. Kisseleff, S. Chatzinotas, and B. Ottersten, "Reconfigurable intelligent surface in challenging environments," Nov. 2020. [Online]. Available: <https://arxiv.org/abs/2011.12110v1>
- [8] M. D. Renzo, A. Zappone, M. Debbah, M. Alouini, C. Yuen, J. Rosny, and S. Tretyakov, "Smart radio environments empowered by reconfigurable intelligent surfaces: How it works, state of research, and road ahead," *IEEE J. Sel. Areas Commun.*, vol. 38, no. 11, pp. 2450-2525, Nov. 2020.
- [9] Y.-C. Liang, R. Long, and Q. Zhang, "Large intelligent surface/antennas (LISA): Making reflective radios smart," *J. Commun. Inf. Networks*, vol. 4, no. 2, pp. 40-50, Jun. 2019.
- [10] C. Pan, et al., "Reconfigurable intelligent surface for 6G and beyond: Motivations, principles, applications and research directions," Nov. 2020. [Online]. Available: <https://arxiv.org/abs/2011.04300v1>
- [11] S. Zhou, W. Xu, K. Wang, M. D. Renzo, and M. Alouini, "Spectral and energy efficiency of IRS-assisted MISO communication with hardware impairments," *IEEE Wireless Commun. Lett.*, vol. 9, no. 9, pp. 1366-1369, Apr. 2020.
- [12] C. Huang, A. Zappone, G. C. Alexandropoulos, M. Debbah, and C. Yuen, "Reconfigurable intelligent surfaces for energy efficiency in wireless communication," *IEEE Trans. Wireless Commun.*, vol. 18, no. 8, pp. 4157-4170, Aug. 2019.
- [13] Q. Wu and R. Zhang, "Intelligent reflecting surface enhanced wireless network via joint active and passive beamforming design," *IEEE Trans. Wireless Commun.*, vol. 18, no. 11, pp. 5394-5409, Nov. 2019.
- [14] X. Yu, D. Xu, and R. Scholar, "MISO wireless communication systems via intelligent reflecting surface," in *Proc. IEEE Int. Conf. Commun. China (ICCC)*, Changchun, China, Aug. 2019.
- [15] P. Wang, J. Fang, L. Dai, and H. Li, "Joint transceiver and large intelligent surface design for massive MIMO mmWave systems," *IEEE Trans. Wireless Commun.*, vol. 20, no. 2, pp. 1052-1064, Oct. 2020.
- [16] Z. Li, M. Hua, Q. Wang, and Q. Song, "Weighted sum-rate maximization for multi-IRS aided cooperative transmission," *IEEE Commun. Lett.*, vol. 9, no. 10, pp. 1620-1624, Jun. 2020.
- [17] H. Li, R. Liu, M. Li, and Q. Liu, "IRS-enhanced wideband MU-MISO-OFDM communication systems," in *Proc. IEEE Wireless Commun. Network Conf. (WCNC)*, Seoul, Korea (South), May 2020.
- [18] D. Zhao, H. Lu, Y. Wang, H. Sun, Y. Gui, and J. Wu, "Joint power allocation and user association optimization for IRS-assisted mmwave systems," *IEEE Trans. Wireless Commun.*, vol. 21, no. 1, pp. 577-590, Jan. 2022.
- [19] Q. Wu and R. Zhang, "Beamforming optimization for wireless network aided by intelligent reflecting surface with discrete phase shifts," *IEEE Trans. Commun.*, vol. 68, no. 3, pp. 1838-1851, Mar. 2020.
- [20] M.-A. Badiu and J. P. Coon, "Communication through a large reflecting surface with phase errors," *IEEE Wireless Commun. Lett.*, vol. 9, no. 2, pp. 184-188, Feb. 2020.
- [21] Y. Liu, J. Zhao, M. Li, and Q. Wu, "Intelligent reflecting surface aided MISO uplink communication network: Feasibility and power minimization for perfect and imperfect CSI," *IEEE Trans. Commun.*, vol. 69, no. 3, pp. 1975-1989, Nov. 2020.
- [22] X. Yu, D. Xu, and R. Schober, "Enabling secure wireless communications via intelligent reflecting surfaces," in *Proc. IEEE Global Commun. Conf. (GLOBECOM)*, Waikoloa, HI, Dec. 2019.
- [23] H. Shen, W. Xu, S. Gong, Z. He, and C. Zhao, "Secrecy rate maximization for intelligent reflecting surface assisted multi-antenna communications," *IEEE Commun. Lett.*, vol. 23, no. 9, pp. 1488-1492, Sep. 2019.
- [24] E. Basar, "Reconfigurable intelligent surface-based index modulation: A new beyond MIMO paradigm for 6G," *IEEE Trans. Commun.*, vol. 68, no. 5, pp. 3187-3196, May 2020.
- [25] Y. Ma, R. Liu, M. Li, and Q. Liu, "Passive information transmission in intelligent reflecting surface aided MISO systems," *IEEE Commun. Lett.*, vol. 24, no. 12, pp. 2951-2955, Dec. 2020.
- [26] S. Abeywickrama, R. Zhang, Q. Wu, and C. Yuen, "Intelligent reflecting surface: Practical phase shift model and beamforming optimization," *IEEE Trans. Commun.*, vol. 68, no. 9, pp. 5849-5863, Sep. 2020.
- [27] J. Y. Lau and S. V. Ham, "A wideband reconfigurable transmitarray element," *IEEE Trans. Antennas Propag.*, vol. 60, no. 3, pp. 1303-1311, Mar. 2012.
- [28] W. Cai, H. Li, M. Li, and Q. Liu, "Practical modeling and beamforming for intelligent reflecting surface aided wideband systems," *IEEE Commun. Lett.*, vol. 24, no. 7, pp. 1568-1571, Apr. 2020.
- [29] H. Li, W. Cai, Y. Liu, M. Li, Q. Liu, and Q. Wu, "Intelligent reflecting surface enhanced wideband MIMO-OFDM communications: From practical model to reflection optimization," *IEEE Trans. Commun.*, vol. 69, no. 7, pp. 4807-4820, Mar. 2021.
- [30] F. Costa and M. Borgese, "Electromagnetic model of reflective intelligent surfaces," *IEEE Open J. Commun. Society*, vol. 2, pp. 1577-1589, Jun. 2021.
- [31] S. Shen, B. Clerckx, and R. Murch, "Modeling and architecture design of intelligent reflecting surfaces using scattering parameter network analysis," Nov. 2020. [Online]. Available: <https://arxiv.org/abs/2011.11362>
- [32] H. Liu, X. Yuan, and Y.-J. A. Zhang, "Matrix-calibration-based cascaded channel estimation for reconfigurable intelligent surface assisted multiuser MIMO," *IEEE J. Sel. Areas Commun.* vol. 38, no. 11, pp. 2621-2636, Nov. 2020.
- [33] D. Mishra and H. Johansson, "Channel estimation and low-complexity beamforming design for passive intelligent surface assisted MISO wireless energy transfer," in *Proc. IEEE Int. Conf. Acoust. Speech Signal Process. (ICASSP)*, Brighton, UK, May 2019.
- [34] Z. Wang, L. Liu, and S. Cui, "Channel estimation for intelligent reflecting surface assisted multiuser communications: Framework, algorithms, and analysis," *IEEE Trans. Wireless Commun.*, vol. 19, no. 10, pp. 6607-6620, Oct. 2020.
- [35] B. Zheng and R. Zhang, "Intelligent reflecting surface-enhanced OFDM: Channel estimation and reflection optimization," *IEEE Wireless Commun. Lett.*, vol. 9, no. 4, pp. 518-522, Apr. 2020.
- [36] W. Yang, H. Li, M. Li, Y. Liu, and Q. Liu, "Channel estimation for practical IRS-assisted OFDM systems," in *Proc. IEEE Wireless Commun. Network Conf. (WCNC) Workshops*, Nanjing, China, Mar. 2021.
- [37] T. V. Chien, H. Q. Ngo, S. Chatzinotas, M. D. Renzo, and B. Ottersten, "Reconfigurable intelligent surface-assisted cell-free massive MIMO systems over spatially-correlated channels," *IEEE Trans. Wireless Commun.*, to appear.
- [38] B. Zheng, C. You, W. Mei, and R. Zhang, "A survey on channel estimation and practical passive beamforming design for intelligent reflecting surface aided wireless communications," *IEEE Commun. Surveys & Tutorials*, to appear.
- [39] A. L. Swindlehurst, G. Zhou, R. Liu, C. Pan, and M. Li, "Channel estimation with reconfigurable intelligent surfaces - A general framework," Oct. 2021. [Online]. Available: <https://arxiv.org/abs/2110.00553>
- [40] B. O. Zhu, J. Zhao, and Y. Feng, "Active impedance metasurface with full 360° reflection phase tuning," *Scientific Reports*, vol. 3, pp. 3059-3064, Oct. 2013.
- [41] L. Dai, B. Wang, M. Wang, and X. Yang, "Reconfigurable intelligent surface-based wireless communication: Antenna design, prototyping and experimental results," *IEEE Access*, vol. 8, pp. 45913-45923, Mar. 2020.
- [42] F. Yang, R. Deng, S. Xu, and M. Li, "Design and experiment of a near-zero-thickness high-gain transmit-reflect-array antenna using anisotropic metasurface," *IEEE Trans. Antennas Propag.*, vol. 66, no. 6, pp. 2853-2861, Jun. 2018.
- [43] T. Van Chien, H. Q. Ngo, S. Chatzinotas, B. Ottersten and M. Debbah, "Uplink Power Control in Massive MIMO with Double Scattering Channels," *IEEE Trans. Wireless Commun.*, vol. 21, no. 6, pp.1989-2005, Mar. 2022.
- [44] M. Grant and S. Boyd, "CVX: MATLAB software for disciplined convex programming," 2016. [Online]. Available: <http://cvxr.com/cvx>
- [45] R. Liu, M. Li, Q. Liu, and A. L. Swindlehurst, "Joint symbol-level precoding and reflecting designs for IRS-enhanced MU-MISO systems," *IEEE Trans. Wireless Commun.*, vol. 20, no. 2, pp. 798-811, Feb. 2021.
- [46] N. Boumal, B. Mishra, P.-A. Absil, and R. Sepulchre, "Manopt, a MATLAB toolbox for optimization on manifolds," *The J. Mach. Learn. Res.*, vol. 15, no. 1, pp. 1455-1459, 2014.
- [47] H. Ding and K.-C. Leung, "Cross-Layer resource allocation in NOMA systems with dynamic traffic arrivals," in *Proc. IEEE Wireless Commun. Network Conf. (WCNC)*, Seoul, Korea, May 2020.
- [48] H. A. Le Thi, T. Pham Dinh, and H. V. Ngai, "Exact penalty and error bounds in DC programming," *J. Global Optimization*, vol. 52, no. 3, pp. 509-535, Mar. 2012.
- [49] Q. Shi, M. Razaviyayn, Z. Q. Luo, and C. He, "An iteratively weighted MMSE approach to distributed sum-utility maximization for a MIMO interfering broadcast channel," *IEEE Trans. Signal Process.*, vol. 59, no. 9, pp. 4331-4340, Sep. 2011.
- [50] 3GPP TR 38.901. "Study on channel model for frequencies from 0.5 to 100 GHz," *3rd Generation Partnership Project; Technical Specification Group Radio Access Network*.